

Activation of Transcription from a Distance:
Investigations on the Oxidation of SoxR by DNA-
Mediated Charge Transport

Thesis by
Paul Eulehwann Lee

In Partial Fulfillment of the Requirements
for the Degree of
Doctor of Philosophy

California Institute of Technology
Pasadena, California
2010
Defended December 21, 2009

ACKNOWLEDGEMENTS

“But there’s no sense crying over every mistake. You just keep on trying ‘till you run out of cake.”

-GLaDOS

First and foremost I would like to thank my research advisor, Prof. Jackie Barton, for her support, guidance, and encouragement during my graduate studies. I have been very fortunate to have had the opportunity to do exciting science in her lab, and I have learned much about what it takes to become a good scientist as well as a good mentor through her example. Throughout the years, I have come to admire and appreciate her zeal for research, her directness and humor, and the care with which she treats her students and postdocs.

Thanks go to my thesis committee, Profs. Harry Gray, Judy Campbell, and Bil Clemons, for their support as well. It is an honor to present my ideas and research to such distinguished faculty, and I appreciate their encouragement and helpful feedback.

There are several collaborators who have contributed to this body of work. First, Prof. Bruce Demple, and his former postdoc Prof. Eunsuk Kim, have kindly provided us with helpful discussion and useful protein. Research presented here was also done in collaboration with Prof. Dianne Newman and her former postdoc Prof. Lars Dietrich.

My experience here at Caltech would not have been a good one had it not been for the members of the Barton group, past and present. Many thanks to those who have trained me: Sarah Delaney, Eylon Yavin, Maria DeRosa, and Eric Stemp. Many thanks to Kate Augustyn for helping my transition into graduate school be a smooth (and delicious) one. Special thanks to my bench buddy Amie Boal for teaching me not only how to grow bacteria, but for being a mentor in various sewing projects as well, and a great workout partner in the pool. Congrats to the other Barton group members of my graduating class, Joey Genereux and Cindy Puckett. I would also

like to thank Eric Olmon for help on transient absorption studies, and for being a cool guy in general. Cheers to the Cake Committee, of which many past and present Barton group members have been a part of.

Special thanks must go to those whose friendship defies context. Brian Zeglis has been my partner in crime for much shenanigans both with the group and on our own. Marisa Buzzeo has been like a big sister to me. Pam Sontz has always been there with her quirky and fun personality when I've needed a confidence boost. Jen and Christian Franck have been fellow cat people and great workout partners. Friends like these remind you, no matter what you are doing, to take joy in life and all its experiences.

Finally, I would have to thank my family for their unending support. My grandmother, Maria Sang-Soon Lee, taught me from a young age to be proud of myself. My parents Bernard and Jae taught me discipline, the value of hard work and a good education, and the importance of seizing opportunity and trying new things. Thanks to my siblings, John, Jeannie, and Tim: you remind me what is really of value in my life. I love you all very much.

ABSTRACT

In enteric bacteria, the cellular response to oxidative stress caused by superoxide is activated by *soxR*, which encodes a redox-active transcription factor that contains a [2Fe2S] cluster and binds DNA with high affinity. Here we describe how SoxR may detect global changes in oxidative stress while bound to DNA at a single location through DNA-mediated charge transport. A unique property of DNA is its ability to delocalize charge along its base stack, allowing oxidative damage to be funneled to specific sites of low oxidation potential. Charge transport also has the potential to access proteins with redox-active moieties.

Electrochemical studies presented here demonstrate that the redox couple of the [2Fe2S] clusters of SoxR can be accessed through the DNA, and that when the protein is bound to DNA, is shifted almost 0.5 V positive to its potential measured in solution in the absence of DNA. SoxR in its reduced form is found to inhibit guanine damage by repairing guanine radicals formed in DNA by the use of various photoactive metallointercalators, by donating an electron from one of its [2Fe2S]⁺ clusters and filling the guanine radical hole. RT-PCR is used to monitor the amount of *soxS* mRNA produced in cells that have taken up the DNA binding photooxidant [Rh(phi)₂bpy]³⁺ and are treated with light. Cells thus treated to generate guanine radicals express *soxS*, evidence that SoxR is being oxidized. An *in vitro* assay is furthermore used to examine directly the DNA-mediated oxidation of SoxR by measuring its transcriptional activity. [Rh(phi)₂bpy]³⁺, tethered to DNA 80 bp from the *soxS* promoter, induces transcription by activating SoxR upon irradiation. These results demonstrate not only that guanine radicals can act to oxidize SoxR, but that the resulting oxidized, DNA-bound protein is biologically active. Thus, transcription can be activated from a distance through DNA-mediated charge transport.

The ability of DNA to conduct charge along its base stack allows offers a general strategy for DNA-mediated signaling of oxidative stress, as it allows information about oxidative events to be transmitted quickly and directly to the proteins responsible for turning on the genes necessary for cell survival.

TABLE OF CONTENTS

Acknowledgements	iii
Abstract	v
Table of Contents	vi
List of Figures and Tables	ix
Chapter 1: SoxR and the Biology of DNA-Mediated Charge Transport	1
Charge transport through B-DNA	2
Biological roles of DNA charge transport	5
Oxidative damage in cells	6
SoxR and the <i>soxRS</i> response to superoxide stress in <i>E. coli</i>	8
References	20
Chapter 2: The Electrochemistry of DNA-Bound SoxR on Gold and Graphite	22
Introduction	23
Charge transport in DNA on a gold electrode	23
Electrochemistry of proteins bound to DNA	24
The electrochemistry of SoxR	25
Results	28
Experimental strategy for SoxR electrochemistry on gold	28
SoxR binding is reported through the Redmond Red electrochemical signal	31
Electrochemistry of <i>P. aeruginosa</i> SoxR	33
Comparison of the voltammetry of <i>E. coli</i> and <i>P. aeruginosa</i> SoxR	36

Discussion	38
Experimental	42
References	46
Chapter 3: Effects of SoxR on the Formation of Guanine Radical	
Induced Damage to DNA	49
Introduction	50
Oxidative damage in cells	50
Ruthenium chemistry	50
The role of guanine radicals in SoxR activation	53
Results	54
Flash quench damage to DNA	54
Damage attenuation with SoxR	57
Discussion	61
Experimental	64
References	67
Chapter 4: Light Induced Transcriptional Activation of the <i>soxS</i>	
Gene in <i>Escherichia coli</i>	68
Introduction	69
Results	73
Discussion	78
Experimental	81
References	84
Chapter 5: <i>In Vitro</i> Transcriptional Activation of <i>soxS</i> from a Distance	
by DNA-Mediated SoxR Oxidation	85

Introduction	86
<i>In vitro</i> transcription assays	87
Troubleshooting transcription assays	88
Transcription studies on SoxR	89
Results	
Guanine oxidation in the 180-mer PCR template DNA	92
Transcriptional activation by SoxR	96
Optimization of transcription assay conditions	96
Comparison of <i>P.aeruginosa.</i> and <i>E. coli</i> SoxR and effect of irradiation	100
Light induced transcriptional activation	100
Discussion	103
Experimental	106
References	109
Chapter 6: Summary and Future Perspectives	110

LIST OF FIGURES AND TABLES

Figure 1.1. Structure of the DNA double helix.	3
Figure 1.2. Examples of DNA-mediated charge transport	4
Figure 1.3. Biological significance of DNA-mediated CT	7
Table 1.1. Genes activated by SoxS	8
Figure 1.4. Primary amino acid comparison of SoxR and MerR	12
Figure 1.5. Comparison of the structures of SoxR and BmrR	13
Figure 1.6. UV-vis and EPR spectra of SoxR	15
Figure 1.7. SoxR footprint region	16
Figure 1.8. Redox-mediated transcriptional activity of SoxR	17
Figure 2.1. Schematic of self-assembly of DNA on electrodes	29
Figure 2.2. Square-wave voltammetry of SoxR on gold	30
Figure 2.3. Electrochemistry of SoxR on graphite	32
Figure 2.4. Binding of SoxR to the DNA-modified electrode.	34
Figure 2.5. Square-wave voltammetry of <i>P. aeruginosa</i> and <i>E. coli</i> SoxR	37
Figure 2.6. Redox potentials of free and DNA-bound SoxR	39
Figure 3.1. The flash-quench scheme	52
Figure 3.2. Guanine oxidation of DNA by different photooxidants/quenchers	55
Figure 3.3. Schematic of the guanine oxidation attenuation experimental system	56
Figure 3.4. Attenuation of guanine damage by SoxR	58
Figure 3.5. Attenuation of guanine damage by SoxR at higher ratios	60
Figure 3.6. Schematic of the results of the G ^{ox} attenuation studies	62
Figure 4.1. Schematic for assaying cells for <i>soxS</i> transcription	71
Figure 4.2. The procedure for reverse-transcriptase PCR (RT-PCR)	72
Figure 4.3. <i>SoxS</i> expression and optical density as a function of [Rh(phi) ₂ bpy]	74
Figure 4.4. Transcript levels of <i>soxS</i> with irradiation time	76

Figure 4.5. Transcript levels of <i>soxS</i> compared to methyl viologen	77
Figure 5.1. Schematized model of transcriptional activation of SoxR from a distance	91
Figure 5.21. Sequence of the 180 base pair transcription template	93
Figure 5.3.: Schematized model for the long range photooxidation of the transcriptional template	94
Figure 5.4. Guanine oxidation of the transcriptional template	95
Figure 5.5. Schematic for the abortive transcription assay	97
Figure 5.6. Gel image of SoxR dependent transcription	98
Figure 5.7. Abortive transcription assay results under different conditions	99
Figure 5.8. Comparison of transcription by <i>P.aeruginosa</i> and <i>E. coli</i> SoxR	101
Figure 5.9. Schematic for the light activated transcription by SoxR	102
Figure 5.10. Results of light activated transcription by SoxR	104

Chapter 1

SoxR and the Biology of DNA-mediated Charge Transport

Charge transport through B-DNA

DNA is a double helix composed of an anionic sugar phosphate backbone surrounding a core of electron-rich aromatic heterocycles, which are the four bases adenine, guanine, cytosine, and thymine. These bases are stacked on top of each other with interbase distance of 3.1 Å, similar to the spacing between sheets in graphite. A cross section of DNA, as shown in figure 1.1 further reveals a well structured π -stack of orbitals down the core of the helix, with the polyaromatic bases lined up perpendicular to the helical axis. The similarity in structure between DNA and graphite formed the basis of the postulate early on, that charge could migrate through the DNA base stack along the network of stacked π -orbitals. Indeed, a large body of work has been done since the elucidation of the double-helical structure of DNA which demonstrates that charge transport through DNA is not only possible, but is highly efficient.

The ability of electrons and holes to access these domains in order to transverse the π -stack of DNA has been well documented, in some cases through distances of up to 200 Å [1]. This phenomenon has been investigated by several methods, some of which are illustrated in figure 1.2. Early studies demonstrated that charge could be transferred through the DNA base stack between two metallointercalators tethered at opposite ends of a strand of duplex DNA [2]. A variety of photooxidants has also been used to oxidize DNA bases many base pairs away from the initial site of metal binding and charge injection [3, 4].

Oxidation of DNA occurs preferentially at guanine residues and multiplets, as this base has the lowest oxidation potential of all four naturally occurring bases [5]. Sequential guanine residues lower the oxidation potential of the DNA further, and the presence of guanine stretches in DNA may serve as thermodynamic sinks to localize DNA damage to certain areas of the genome [6, 7].

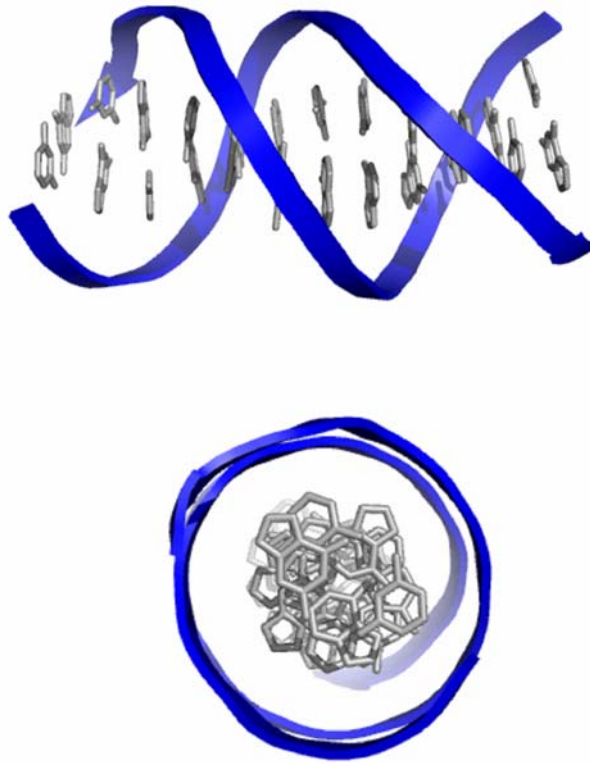


Figure 1.1. Top: A side view of DNA shows the double helical structure of double-stranded DNA and the alignment of adjacent base pairs. Bottom: A cross-sectional view of DNA shows that the bases stack on top of each other, creating a core of delocalized π -bonds.

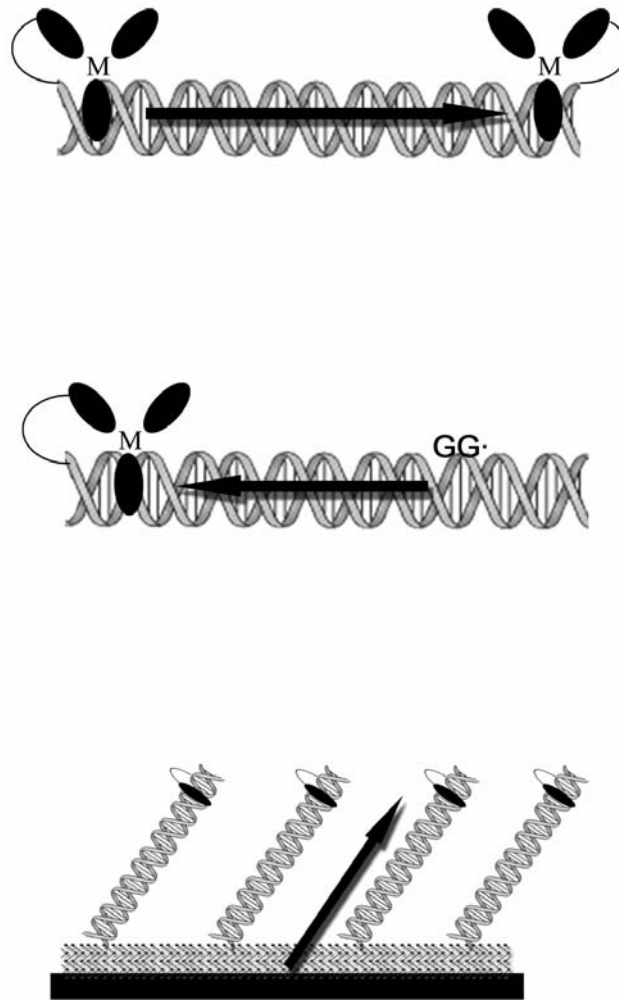


Figure 1.2. Shown here are examples of DNA-mediated charge transport. Top: The photoirradiation of a metal complex allows it to reduce a distally bound complex through the DNA. Middle: A bound photooxidant is able to oxidize DNA bases at a distance. Bottom: DNA on a gold electrode can be used as a medium to monitor the reduction and oxidation of a bound redox probe.

The DNA π -stack has also been used as a medium to electrochemistry. Thiol modified DNA can be attached to a gold electrode surface, and the reduction and oxidation of various DNA-bound redox indicators can be monitored using various electrochemical techniques such as cyclic and square wave voltammetry, and chronocoulometry. These experiments demonstrate that DNA conduction of charge through DNA can occur at energies below the oxidation potential of the bases (8).

Charge transport through DNA has well characterized properties. First, the efficiency of charge separation has a very shallow distance dependence (9). Second, the rate of charge migration through DNA is very rapid, with rates on the order of 10s to 100s of picoseconds (10). Finally, DNA charge transport is extremely sensitive to the integrity of the base stack, as any perturbations, such as mismatches, abasic sites, or oxidative lesions will serve as barriers to charge migration (11,12).

Biological roles of DNA charge transfer

Given the robust nature of charge transport through DNA, it would be surprising if organisms had not evolved ways to utilize this chemistry (figure 1.3) Of particular interest is the ability of DNA-bound proteins that contain a redox-active moiety, such as a disulfide bond or [FeS] cluster, to couple into the electronics of the DNA base stack, allowing them to exchange electrons or holes with the DNA and become reduced or oxidized in the process.

Long range oxidation and reduction in a DNA-mediated manner has been demonstrated electrochemically for proteins bound to DNA on a gold surface. This method has enabled the direct measurement of the redox potentials for the [4Fe4S] cluster containing glycosylases MutY and EndoIII (13, 14). In both of these cases, it was found that binding to DNA shifts the potential of the cluster to a more biologically relevant range. This technique has also allowed the direct monitoring of enzymatic processes of DNA bound proteins, as in the case of photolyase, where the redox state of the flavin cofactor was monitored as it repaired a thymine dimer (15).

The ability of proteins to accept and donate electrons through the base stack, along with the fact that DNA is extremely sensitive to base lesions and mismatches, provides an explanation for how DNA repair enzymes are able to locate their substrates rapidly despite their low copy number in the cell (16). In this model, a repair enzyme will processively scan DNA until a second enzyme binds some distance away and sends an electron into the base stack. If the DNA between the two enzymes is intact, the electron is able to travel to the first enzyme, reducing it and causing it to dissociate from the DNA. However, if there is a base lesion between the two enzymes, charge transport between the enzymes will not occur, and the first enzyme will continue scanning until it eventually reaches the site of the lesion. In this manner, enzymes will not waste time slowly interrogating intact DNA, and there will be a net redistribution of repair enzymes away from “healthy” regions of DNA and toward DNA which contains lesions.

DNA-bound proteins can also be oxidized by guanine radicals in DNA, formed as a result of reactive oxygen species in the cell, or *in vitro* by photooxidants as described previously. Oxidation of a protein using photooxidants in a DNA-mediated manner has been observed for MutY, which is able to compete with guanine residues for holes (17). P53, which contains several redox-active cysteine residues, also be oxidized this way, forming disulfide bonds and causing the protein to dissociate from the promoter regions of some of its target genes (18). Importantly, the formation of guanine radicals in DNA is an indicator of oxidative DNA damage and possibly oxidative conditions in the cell; the rapid migration of these holes allows proteins to detect damage conditions rapidly and induce the proper cellular response.

Oxidative damage in cells

Reactive oxygen species (ROS) are a normal by-product of respiration in cells, and can arise when molecular oxygen (O₂) reacts with radical intermediates in the electron transport chain. ROS concentration in healthy cells is maintained at low levels of around 10⁻⁹ M for superoxide

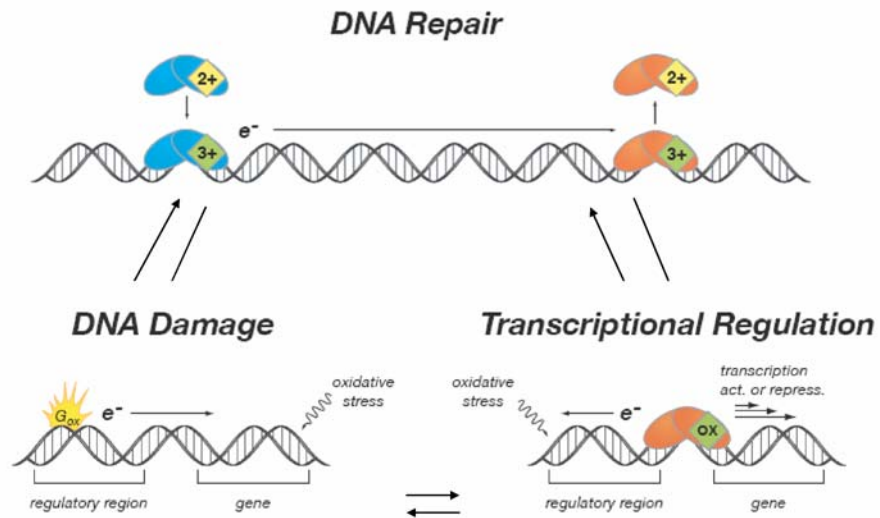


Figure 1.3. DNA-mediated charge transport has biological significance. Repair proteins may be able to scan long regions of the DNA for their substrate. DNA damage can be funneled to specific regions of the genome. Oxidative radicals, an early sign of oxidative stress in the cell, can be detected by transcription factors, which then activate regulatory genes.

($O_2^{\cdot-}$), mainly through superoxide dismutase (SOD) which converts $O_2^{\cdot-}$ into H_2O_2 . Hydrogen peroxide (H_2O_2) is maintained at 10^{-8} M in cells mainly through catalase, which converts peroxide to H_2O and O_2 . However, the levels of these species can be elevated in a variety of ways.

Hyperbaric oxygen can increase the rate of collision of O_2 with various respiratory proteins, and antibiotics that interfere with the respiratory electron transfer chain can increase the amounts of reactive intermediates. Various redox cycling drugs can generate ROS in the cytoplasm, and H_2O_2 is used as a chemical weapon by organisms such as macrophages and amoeba (19).

On their own, $O_2^{\cdot-}$ and H_2O_2 are relatively unreactive. Superoxide does most damage to proteins containing iron-sulfur clusters, such as aconitase, for which it oxidizes the 4Fe4S cluster, which then loses an iron and falls apart. H_2O_2 is able to damage certain sulfur moieties in proteins. The real danger behind these reactive species is in the Fenton reaction, during which free Fe(III) reacts with H_2O_2 to form destructive hydroxyl radicals ($HO\cdot$), which, unlike superoxide, is able to permeate cellular membranes and attack a variety of biochemicals, most significant of which is DNA. Importantly, $O_2^{\cdot-}$ stands out as a particularly insidious species as it both increases the amount of free Fe in the cell and is a source of H_2O_2 by its own dismutation (19).

SoxR and the soxRS response to superoxide stress in E. coli

The cell has different responses to $O_2^{\cdot-}$ versus H_2O_2 . The main regulator of H_2O_2 induced oxidative stress is the OxyR regulon; OxyR is a transcriptional activator that senses H_2O_2 levels in the cell by the formation of a disulfide bridge between two of its cysteine residues (20).

However, constitutive induction of this OxyR is not sufficient to protect cells against redox cycling agents that produce $O_2^{\cdot-}$. The two oxidants have been shown to induce different DNA damage responses, and unlike H_2O_2 , $O_2^{\cdot-}$ induced stress does not trigger the SOS response. The protein expression profiles are also different when comparing the two stressors. However, some differences in protein expression were observed when comparing the protein expression profiles

Table 1.1. Genes activated as part of the *SoxRS* operon

Uptake	<i><u>fur</u></i> : iron uptake repressor <i><u>marA</u></i> , <i><u>araAB</u></i> : drug resistance and efflux pumps
DNA associated	<i><u>dps</u></i> : stress response DNA binding protein <i><u>nfo</u></i> : Endonuclease IV <i><u>dnaE</u></i> : α -subunit of DNA polymerase III
Redox enzymes	<i><u>cyoD</u></i> , <i><u>ccmD</u></i> : cytochrome C related <i><u>sodA</u></i> : Mn superoxide dismutase
Cellular reduction	<i><u>fpr</u></i> : NADP ⁺ reductase <i><u>nuoIK</u></i> : NADH hydrogenase <i><u>zwf</u></i> : glucose 6 phosphate dehydrogenase <i><u>pgi</u></i> : glucose phosphate isomerase

The genes activated by SoxR help the cell mitigate conditions of oxidative stress, and can be grouped into four functions: (1) regulating the uptake and efflux of iron and drugs by various membrane pumps, (2) upregulating proteins that help protect and repair DNA, (3) inactivation of reactive oxygen species by reaction with redox enzymes, and (4) restoring and maintaining the reductive environment inside the cell. The most well-characterized genes are shown here with their functions.

of *E. coli* lacking any superoxide dismutase (SOD) activity and wild type *E. coli* treated with the redox cycling agents paraquat and plumbagin (21).

Genome-wide mutational analysis was used to identify the regulon responsible for the unique $O_2^{\cdot -}$ response in *E. coli* (22, 23). This regulon, named *soxRS* (superoxide response) is comprised of two genes: *soxR*, which encodes a 17 kDa, 154–amino acid transcription factor which operates as a homodimer, and its target gene *soxS*, which encodes as 13 kDa transcription factor (24). SoxR operates from a single site on the genome, at the *soxS* promoter containing a palindromic recognition element and allosterically downregulates its own expression by acting as a repressor at its own promoter site. This downregulation results in a low copy number of SoxR in the cell (<100 nM) (25). The promoter region is characterized by an 18–base pair palindromic recognition element, and the footprint of SoxR on the promoter region stretches 36–base pairs long.

Under conditions of oxidative stress, SoxR is able to activate transcription of *soxS*, increasing its mRNA levels to ~100× that of unstressed cells (26). Once expressed, SoxS is able to turn on the transcription of several dozen genes that help the cell mitigate the effects of oxidative stress (27). These genes include regulators of iron uptake, a Mn-only SOD, endonuclease IV (which is involved in repair of abasic sites), and several genes that help to restore the reducing environment within the cell (Table 1). Once the threat of oxidative damage has passed, SoxR is rapidly re-reduced in the cell, turning off transcription of SoxS; as of yet, the cellular factor(s) responsible for reducing SoxR have not been characterized. SoxS is rapidly degraded in the cell, and the *soxS* mRNA has a half-life of approximately one minute (28).

The SoxR/SoxS paradigm is only true for enterics. Though SoxR analogues have also been identified in bacteria which lack SoxS, in these species, SoxR binds to multiple sites on the genome and directly activates a variety of genes with different functions. Furthermore the role of SoxR can diverge from that of responding to elevated levels of $O_2^{\cdot -}$ in the cell. In these

organisms, agents other than $O_2\cdot$ are able to activate SoxR, and in some cases, deletion of the *soxR* gene has no effect on $O_2\cdot$ resistance (29).

SoxR is a member of the MerR family of transcription factors, which includes ZntR, and CueR, which sense Zn(II) and Cu(II) respectively. These proteins share a common homology; they all function as homodimers, and each subunit contains a C-terminal metal-binding domain that is specific for a unique metal, a dimerization interface, and an N-terminal helix-turn-helix DNA binding domain (30, 31). The mode of action is also conserved; these proteins bind in the region of the promoter usually bound by repressors, and the spacing between the -10 and -35 conserved boxes in the promoters of their gene targets is longer than the 17–base pair consensus spacing optimal for RNA polymerase binding. Upon metal binding the protein induces a large conformational change in the DNA, which allows RNA polymerase to bind and transcribe the target gene. Figure 1.4 shows the primary amino acid sequence comparison of SoxR with MerR, and Figure 1.5 shows a structural comparison of SoxR with BmrR, another member of the MerR family.

However, unlike the other members of the MerR family, SoxR contains a redox-active [2Fe2S] cluster in place of a metal- or drug-binding domain, which is crucial for its activity, but is not important structurally. There is one cluster per monomer of SoxR, ligated by four cysteine residues (Cys-119, Cys-122, Cys-124, and Cys-130) (32). This cluster is known to exist in two oxidation states, the reduced [2Fe2S]⁺ form and the oxidized [2Fe2S]²⁺ form. Reduced SoxR is EPR active, and has signals with *g*-values of 2.01, 1.92, and 1.90; oxidized SoxR is EPR silent. The two forms of the protein also have different UV-vis spectra. The oxidized form of the protein has bands with the following mM⁻¹ extinction coefficients: $\epsilon_{276} = 53.5$, $\epsilon_{320} = 24.5$, $\epsilon_{418} = 12.7$, $\epsilon_{462} = 12.4$, $\epsilon_{540} = 8.0$; reduced SoxR retains the peak at 276 nm, but lacks the iron sulfur bands between 320 and 540 nm. The EPR and UV-vis characterization of SoxR are shown in Figure 1.6, and these are consistent with the cluster being a [2Fe2S] cluster (33).

```

MerR      MEKNLEN---LTIGVFAKAAGVNVETIRFYQRKGLLPEPDKPYGSIRRYGEADVTRVRF 56
SoxR      MEKKLPRIKALLTPGEVAKCSGVAVSALHFYESKGLITSIRN-SGNQRRYKRDVLRVAI 59
          ***:* .   ** * .**.* ** *.:**:* ***:.. : *. *** . : * :

MerR      VKSAQRLGFSLDEIAELLRLDDGTH--CEEASSLAEHKLQDVREKMTDLARMETVLSSEL 113
SoxR      IKIAQRIGIPLATIGEAFGLPEGHTLSAKEWKQLSSQWREELDRRIHTLVALRDELDGC 119
          :* ***:*:* *.* : : * .:* ..*:.: ::: :. :* .: .*.

MerR      VFACHARQGNVSCPLIASLQGEKEPRGADAV----- 144
SoxR      IGCGCLSRSDCPLRNPGDRLGE-EGTGARLLEDEQN 154
          : .   :.: .   .. ** * ** :

```

Figure 1.4. SoxR is in the MerR family of transcriptional activators. Shown here is a primary amino acid sequence alignment of the Hg(II)-sensing protein MerR with that of SoxR. Asterisks (*) indicate amino acid identity, colons (:) indicate conserved substitutions, and periods (.) indicate semiconserved substitutions. The DNA binding domain is highlighted in green, the dimerization domain is highlighted in blue, and the metal binding residues are shown in bold type. SoxR contains four cysteine residues which ligate a [2Fe2S] cluster. The alignment was generated using ClustalW2 (<http://www.ebi.ac.uk/Tools/clustalw2/index.html>).

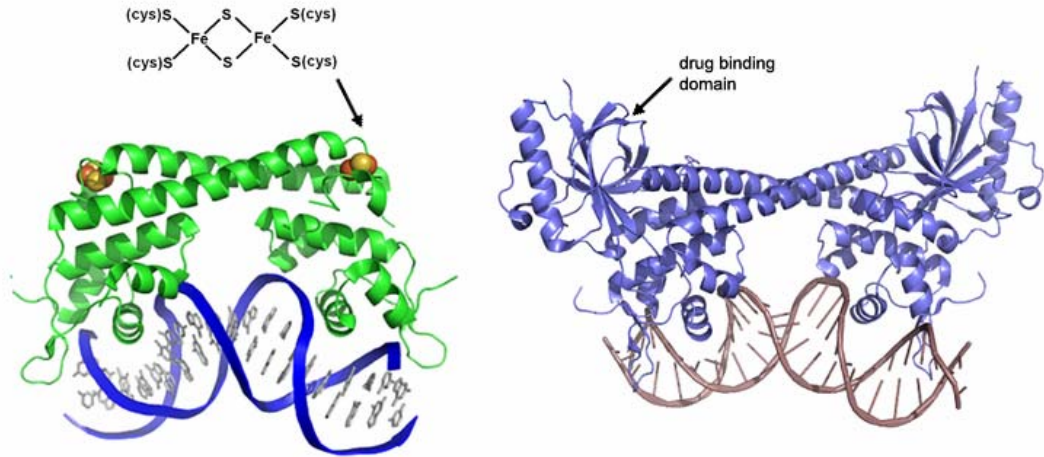


Figure 1.5. Oxidized SoxR (left) and BmrR bound to the drug TPP (right) are both in the MerR family of transcriptional activators. Both share strongly homologous helix-turn-helix DNA binding domains and α -helices in the dimerization domain. However, BmrR contains a large drug binding domain that is absent in SoxR, and replaced by [2Fe2S] clusters.

In cells, the clusters of SoxR are maintained in a reduced $[2\text{Fe}_2\text{S}]^+$ state (34), and a one electron oxidation of a cluster to the oxidized $[2\text{Fe}_2\text{S}]^{2+}$ state allows SoxR to function as a transcriptional activator (35, 36). Importantly, the cluster is not critical for DNA binding, and apo-SoxR binds DNA with comparable affinity to the intact protein ($K_d = 4.5 \times 10^{-10}$ M) both in its reduced and oxidized forms (28, 33). Thus, SoxR remains bound to the promoter region of its target gene in its inactive state. The binding site and footprint region of SoxR on the *soxS* promoter is shown in Figure 1.7.

SoxR acts as a transcriptional activator by changing the conformation of DNA at its binding site, as illustrated in figure 1.6. The *soxS* promoter region contains a 19–base pair spacing between the conserved promoter boxes, which corresponds to a 6.8 \AA increase in translational length and a rotation of 72° around the axis compared to the consensus 17–base pair spacing. SoxR itself is not thought to interact with RNA polymerase directly; instead, the elongated spacer regions described here preclude binding of RNA polymerase and initiation of transcription even in the absence of SoxR (37, 38). A recently solved crystal structure of the oxidized form of SoxR bound to DNA shows that the transcriptionally active form of the protein induces a 65° bend, as shown in Figure 1.8, and partial unwinding of the DNA at the promoter site, which results in a shortening of the length of the region by 3.4 \AA , or 1 base pair. This change enables RNA polymerase to bind and initiate transcription (39).

Although the structure of oxidized SoxR is known, in the absence of a corresponding structure for the reduced protein, it is difficult to predict how SoxR is able to induce such a large conformational change in the DNA at its binding site. There is, however, evidence among other members of the MerR family that this change involves a change in the solvent accessibility of one or more of the metal binding centers. The crystal structure of Cu(I) bound to the CueR (copper response) dimer shows one metal ion bound in a solvent inaccessible pocket and another bound at the equivalent site in a disordered fashion (40). The crystal structures of the apo- and drug-bound forms of BmrR reveal that significant disordering of an α -helix occurs in the protein upon drug

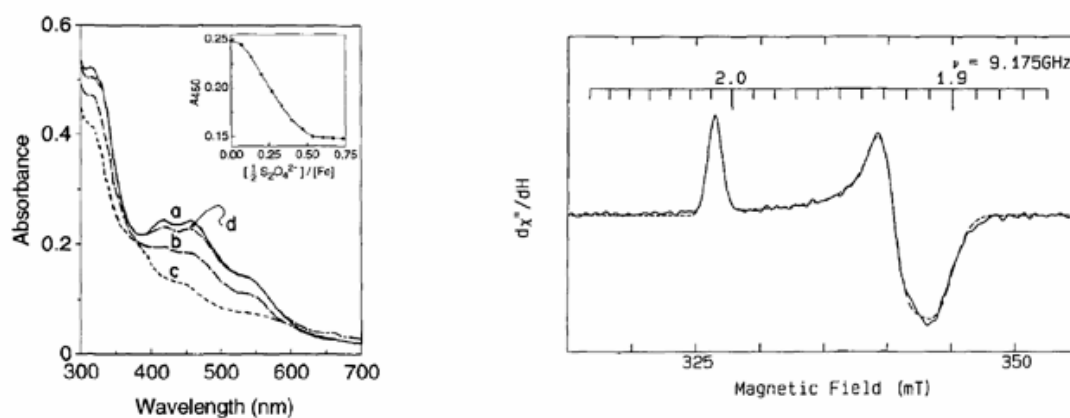


Figure 1.6. Left: Oxidized SoxR has a characteristic UV-vis spectrum for an [FeS] cluster containing protein. The oxidized protein has bands with the following mM⁻¹ extinction coefficients: $\epsilon_{276}=53.5$, $\epsilon_{320}=24.5$, $\epsilon_{418}=12.7$, $\epsilon_{462}=12.4$, $\epsilon_{540}=8.0$; reduced SoxR retains the peak at 276 nm, but lacks the iron sulfur bands between 320 and 540 nm. Right: Reduced SoxR has an EPR spectrum has peaks with g values at 1.93, 1.92, and 2.01. Oxidized SoxR is EPR silent. Taken from Ref. 35.

5'- TTT *TAT AAA CCG CTT TAC CTC AAG TTA ACT TGA GGA ATT A* -3'
 3'- AAA ATA TTT *GGC GAA TTG GAG TTC AAT TGA ACT CCT TAA T* -5'

Figure 1.7. SoxR binds to the soxS promoter region with high affinity. Shown in red is the SoxR footprint; the protein protects 36 bases on one side of the binding site and 25 bases on the other. The palindromic recognition element is shown in italics.

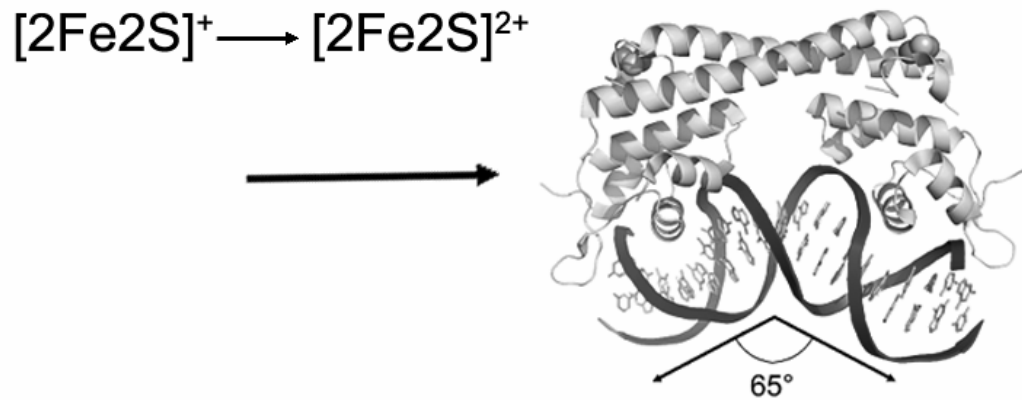


Figure 1.8. The transcriptional activity of SoxR is mediated by its [FeS] clusters. The one-electron oxidation of one of the [2Fe2S] clusters from the +1 state to the +2 state induces a conformational change in the DNA at the promoter site of *soxS*, the target gene for SoxR. The protein induces a 65° bend in the DNA, which amounts to a ~1–base pair shortening of the length of the region between the -10 and -35 promoter elements. This shortening of the spacer region allows RNA polymerase to bind to the promoter and transcribe *soxS*.

binding and activation (41). For oxidized SoxR, the binding region for the [2Fe2S] cluster is fairly solvent accessible, and reduction of these clusters may cause them to become more buried within the protein.

It is well established that SoxR is activated in the presence of redox cycling drugs that form the reactive oxygen species $O_2^{\cdot-}$ but the exact nature of SoxR oxidation is also not known. In fact, SoxR has been reported to be activated by H_2O_2 and NO^{\cdot} as well (42, 43). However, the low copy number of this protein in the cell and the fact that it binds to a single site on the genome with high affinity makes it unlikely that a diffusible species is responsible for oxidizing the iron-sulfur clusters of SoxR. Furthermore, $O_2^{\cdot-}$ is likely to irreversibly degrade the cluster of SoxR upon direct interaction. An alternate hypothesis is that these redox cycling agents interfere with the ability of the cell to maintain SoxR in a reduced state by consuming reducing equivalents to form $O_2^{\cdot-}$ from O_2 ; the same scenario might arise in cells undergoing oxidative stress. Common cellular redox buffers such as glutathione do not reduce SoxR, nor do redox cofactors such as NADPH or NADH. Recently, a possible reducing system for SoxR was identified as the *rsxABCDGE* operon, which shares homology with the *rnf* operon in *Rhodobacter capsulatus* involved in nitrogen fixation; the gene products of this operon have not been well characterized and a direct interaction with SoxR has not been demonstrated (44).

Of particular note is that arguably the most deleterious effect of increased $O_2^{\cdot-}$ levels in organisms is DNA damage caused by the increase in free iron levels and the subsequent production of hydroxyl radicals (OH^{\cdot}). A major product of OH^{\cdot} induced DNA damage are persistent oxidative radicals of the aromatic bases, which, when trapped, lead to permanent oxidative damage products (45). These radicals are able to migrate through the base stack of DNA and between DNA and associated proteins or small molecules, localizing at low oxidation potential sinks. In DNA, these sinks are guanine multiplets, and for proteins, they may be thiol residues or metal clusters (46).

The ability of DNA to conduct charge provides a mechanism for SoxR activation which circumvents the limitations of having a diffusible signal. In this model, the DNA base radicals that are formed when $O_2^{\cdot-}$ levels are elevated in the cell are able to migrate long distances through the DNA to guanine multiplets. These relatively long lived radicals would then be able to oxidize the [2Fe2S] cluster of SoxR from the +1 to the +2 state, causing it to activate the transcription of *soxS*. In this way, information about oxidative events occurring distal to the site of sensor binding can be transmitted across long distances rapidly and induce the desired cellular response. The following studies attempt to address this mechanism for SoxR activation by investigating its electrochemical properties, its ability to accept holes in DNA, its ability to activate transcription both *in vitro* and in cells, and the rate of cluster oxidation by DNA-mediated methods.

REFERENCES

1. Nunez, M. E., Hall, D. B., Barton, J. K. *Chem. Biol.* 6:85–97 (1999).
2. Arkin, M. R. et al. *Science* 273:475–480 (1996).
3. Arkin, M. R. et al. *Chem. Biol.* 4:389–400 (1997).
4. Kelley, S. O., Barton, J. K. *Science* 283:375–381 (1999).
5. Steenken, S., Jovanovic, S. V. *J. Am. Chem. Soc.* 119:617–618 (1997).
6. Saito, I. et al. *J. Am. Chem. Soc.* 117:6406–6407 (1995).
7. Merino, E. J., Barton, J. K. *Biochemistry* 46:2805–2811 (2007).
8. Gorodetsky, A. A., Buzzeo, M. C., Barton, J. K. *Bioconj. Chem.* 19:2285–2296 (2008).
9. Augustyn, K. E., Genereux, J., Barton, J. K. *Angew. Chem. Int. Edit.* 46:5731–5733 (2007).
10. Wan, C. et al. *Proc. Natl. Acad. Sci. USA* 97:14052–14055 (2000).
11. Boon et al. *Nat. Biotech.* 18:1096–1100 (2000).
12. Bhattacharya, P. K., Barton, J. K. *J. Am. Chem. Soc.* 123:8649–8656 (2001).
13. Boal, A. K., et al. *Biochemistry* 44:8397–8407 (2005).
14. Gorodetsky A. A., Boal, A. K., Barton, J. K. *J. Am. Chem. Soc.* 128:12082–12083 (2006).
15. DeRosa, M. C., Sancar, A., Barton, J. K. *Proc. Natl. Acad. Sci. USA* 102:10788–10792 (2005).
16. Boal, A. K. et al. *Proc. Natl. Acad. Sci. USA* 106:15237–15242 (2009).
17. Yavin, E., et al. *Proc. Natl. Acad. Sci. USA* 102:3546–3551 (2005).
18. Augustyn, K. E., Merino, E. J., Barton, J. K. *Proc. Natl. Acad. Sci. USA* 104:18907–18912 (2007).
19. Imlay, J. A., *Annu. Rev. Microbiol.* 57:395–418 (2003).
20. Lee, C. et al. *Nat. Struct. Mol. Biol.* 11:1179–1185 (2004).
21. Walkup, L. K., Kogoma, T. *J. Bact.* 171:1476–1484 (1989).
22. Greenberg, J. T. et al. *Proc. Natl. Acad. Sci. USA* 87:6181–6185 (1990).

23. Tsaneva, I. R. and Weiss, B., *J. Bact.* 172:4197–4205 (1990).
24. Wu, J. Weiss, B., *J. Bact.* 173:2864–2871 (1991).
25. Hidalgo, E.; Leautaud, V., Demple, B. *EMBO J.* 17:2629–2636 (1998).
26. Ding, H. Demple, B. *Proc. Natl. Acad. Sci. USA* 94:8445–8449 (1997).
27. Imlay, J. A. *Annu. Rev. Biochem.* 77:755–776 (2008).
28. Hidalgo E., Demple, B. *EMBO J.* 13:138–146 (1994).
29. Dietrich, L., Teal, T., Price-Whelan, A., Newman, D. K. *Science* 321:1203–1206. (2008).
30. Amábile-Cuevas C. F., Demple B. *Nucleic Acids Res.* 19:4479–4484 (1991).
31. Brown, N., Stoyanov, J., Kidd, S., Hobman, J. *FEMS Microbiol. Rev.* 27:145–163 (2003).
32. Gaudu, P., Moon, N., Weiss, B. *J. Biol. Chem.* 272:5082–5086 (1997).
33. Wu, J., Dunham, W. R., Weiss, B. *J. Biol. Chem.* 270:10323–10327 (1995).
34. Gaudu, P., Weiss, B. *Proc. Natl. Acad. Sci. USA* 93:10094–10098 (1996).
35. Hidalgo, E., Demple, B. *J. Biol. Chem.* 271:7269–7272 (1996).
36. Ding, H., Hidalgo, E., Demple, B. *J. Biol. Chem.* 271:33173–33175 (1996).
37. Brown, N. et al. *FEMS Microbiol. Rev.* 27:145–163 (2003).
38. Hidalgo, E., Demple, B. *EMBO J.* 16:1056–1065 (1997).
39. Watanabe, S., Kita, A., Kobayashi K., Miki, K., *Proc. Natl. Acad. Sci. USA* 105:4121–4126 (2008).
40. Changela, A. et al. *Science* 301:1383–1387 (2003).
41. Zheleznova, E., Markham, P., Neyfakh, A., Brennan, R. *Cell* 96:353–362 (1999).
42. Nunoshiba, T., et al. *Proc. Natl. Acad. Sci. USA* 90:9993–9997 (1993)
43. Machado, M.; Michan, C., Pueyo, C. *J. Bacteriol.* 182:6842–6844 (2000).
44. Koo, M. S. et al. *EMBO J.* 22:2614–2622 (2003)
45. Burrows C. J., Muller, J. G. (1998) *Chem. Rev.* 98:1109–1151.
46. Delaney, S., Barton, J. K. (2003) *J. Org. Chem.* 68:6475–6483

Chapter 2

The Electrochemistry of DNA-Bound SoxR on Gold and Graphite

Adapted from Gorodetsky, et al., *Proc Natl Acad Sci USA* 105:3685–3689 (2008).
Experiments on graphite were performed by A. Gorodetsky

INTRODUCTION

Charge transport in DNA on a gold electrode

The ability of DNA to conduct charge is well demonstrated in applications for which it can be used as the conduit between an electrode surface and a DNA-coupled redox active species. Devices that take advantage of DNA in this manner consist of a gold or graphite electrode, onto the surface of which thiol- or pyrene-modified DNA is attached. The DNA and electrode are usually separated by a saturated alkane linker moiety. The electrode is then backfilled with free alkane thiol, which passivates the surface and prevents unspecific non-DNA-mediated interactions between the electrode and any soluble species bound to DNA from occurring (1).

In most cases cyclic voltammetry is used to observe the redox signals of the molecule of interest; in this detection method the potential of the working electrode is scanned across a potential window, and current to and from the electrode surface to the molecule is measured versus the applied potential. This results in a signal shape with a characteristic “duck” shape and two distinct anodic and cathodic peaks for the oxidation and reduction, respectively, of the DNA bound species.

Another electrochemical technique used with DNA-modified electrodes is square wave voltammetry, in which the potential is stepped alternating between negative and positive potentials, which effectively measures the absolute current flow at a given potential for both the anodic and cathodic currents. Square wave voltammetry has the advantage of being a more sensitive technique than cyclic voltammetry, but at the cost of losing information about the specifics of peak height and area, which are important when studying nonreversible and quasi-reversible electrochemical systems.

These techniques have been applied to a variety of redox probes, which are coupled to the base stack of DNA either by intercalation or through a conjugated linker. These signals are largely reversible (except in the case of probes that undergo electrocatalysis), and occur at similar potentials to the non-DNA associated molecule.

Importantly, charge transport to the probe is critically dependent on the nature of the DNA on the surface; specifically, on mismatches and oxidative lesions, which disrupt the base pair stacking. If such a lesion is located on the DNA between the electrode and the probe, charge migration cannot occur and the redox signal from the probe will be greatly attenuated.

Electrochemistry of proteins bound to DNA

DNA-modified electrodes have previously been explored for the study of DNA-mediated charge transport chemistry (2-4). Typically, self-assembled DNA monolayers on gold or graphite are interrogated electrochemically with the efficiency of charge transfer to an electroactive probe yielding information on the integrity of the intervening base pair stack. In fact, duplexes that are covalently modified with redox-active reporters at a fixed position provide particularly well-defined systems for study of DNA charge transport at electrode surfaces, allowing for the electrochemical detection of even small perturbations in the intervening base stack (5-8).

Similar to the detection of redox probes, the potentials of DNA-bound proteins can be measured using the same electrochemical techniques. DNA-modified electrodes have proven highly useful for probing of redox centers within proteins bound to DNA, and have been used to probe the redox potential of MutY and Endo III, base excision repair glycosylases that contain a [4Fe-4S] cluster (9-11). Initial studies of these enzymes had found no clear role for the clusters because, in the absence of DNA, they did not display redox activity within a physiologically relevant range of potentials (12-14). However, at DNA-modified gold surfaces, these BER enzymes display reversible, DNA-mediated electrochemistry with midpoint potentials of ~90 mV (10). Moreover, experiments comparing directly the electrochemistry of Endo III on bare and DNA-modified graphite demonstrated that binding to DNA shifts the redox potential of Endo III by about -200 mV into a physiologically relevant range, activating the cluster for oxidation (11). DNA binding thus changes the redox properties of the enzymes from being similar to ferredoxins to instead resembling high-potential iron proteins. Based on these data, a redox role for the

[4Fe4S] clusters in long-range DNA-mediated signaling has been proposed to detect damaged sites that are to be repaired in the genome (9-11, 15). The ability to alter the redox states of these proteins in a DNA-mediated manner further suggests that DNA may be a medium through which oxidation/reduction reactions occur. This idea of long range DNA-mediated signaling may also be important to consider in the context of SoxR.

The electrochemistry of SoxR

SoxR belongs to the MerR family of transcriptional regulators. The members of this family are defined by an N-terminal helix-turn-helix DNA-binding motif, a coiled-coil dimerization region, and a C-terminal sensory domain (16-18). Although the DNA-binding and dimerization regions are conserved among MerR-type regulators, their sensory domains are diverse (17). Typically, MerR type transcription factors occupy suboptimally spaced 19 ± 1 bp promoter elements in the inactivated state, often inducing a slight bend of the promoter DNA. Upon activation, they are thought to undergo a conformational change that unwinds and bends the promoter region, thereby allowing RNA polymerase to bind and initiating transcription (17).

SoxR regulates an oxidative stress response to superoxide in the enterics *Escherichia coli* and *Salmonella typhimurium* (19, 20). This unique transcription factor is a 17 kDa polypeptide that binds DNA as a dimer and contains a [2Fe2S] cluster in each monomer (19). Loss of this cluster does not affect protein folding, DNA binding, or promoter affinity (21-25), but oxidation of this cluster by either oxygen or superoxide generating agents (e.g., methyl viologen) triggers expression of the transcription factor SoxS (23, 24). Subsequently, SoxS controls the expression of more over 100 genes in the SoxRS regulon which collectively act to repair or avoid oxidative damage (25).

The role of SoxR appears to vary drastically across organisms. Whereas SoxR is conserved in both Gram-negative and Gram-positive bacteria, *soxS* is exclusively found in enterics, indicating that SoxR can be part of different regulatory networks (26, 27). Indeed,

Pseudomonas putida and *P. aeruginosa* do not rely on SoxR for an oxidative stress response (28, 29). Instead, *P. aeruginosa* SoxR responds to phenazines, endogenous redox-active pigments, and activates transcription of two probable efflux pumps and a putative monooxygenase (30) that might aid in phenazine transport and modification. Considering that SoxR shows functional diversity between pseudomonads and enterics, it is surprising that the transcription factor is biochemically conserved: (i) Expression of *P. putida* SoxR in *E. coli* can complement a *soxR* deletion mutant (29) and (ii) the redox potentials of soluble SoxR from *E. coli* and *P. aeruginosa* *in vitro* are both approximately -290 mV vs NHE (22, 23, 30).

The fact that SoxR requires oxidation for its transcriptional activity seems biologically reasonable but also leads to a conundrum. Under normal physiological conditions, it is assumed that SoxR is kept in its reduced, inactive state by the intracellular NADPH/NADP⁺ redox potential of ~340 mV vs NHE (31, 32). Furthermore, it has been reported that NADPH-dependent SoxR reduction is enzyme mediated, allowing for a rapid adjustment to changes in cellular conditions, though direct enzymatic interaction with *soxR* has not yet been demonstrated (33, 34). The conundrum does not lie in the mechanism of SoxR reduction but rather in the specificity of its oxidation: at a low redox potential of -290 mV, many cellular oxidants could react with SoxR, in particular glutathione (35), and therefore SoxR would primarily be in the oxidized form even in the absence of oxidative stress, contrary to studies showing that the protein in cells is strongly reduced. How is SoxR then maintained in its reduced and transcriptionally silent form?

The mechanism underlying the oxidation/activation of SoxR is also not well understood. For *E. coli* SoxR, it was first suggested that superoxide directly oxidizes the iron-sulfur cluster (36, 37). Alternatively, the redox state of SoxR might be coupled to changes in the equilibrium of biologically relevant redox couples, such as NADPH or glutathione (31, 38). Recently, it was shown that the activation of SoxR in *P. aeruginosa* can occur in an oxygen independent manner (29). Considering that both *E. coli* and *P. aeruginosa* SoxR can transfer electrons to the acceptor

safranin O, a phenazine derivative (22, 23, 30), it seems reasonable that endogenous phenazines may oxidize SoxR in pseudomonads. Alternatively, given that pseudomonad phenazines can also modulate the intracellular NADH/NAD⁺ ratio, the possibility that phenazines activate SoxR indirectly must also be considered (39).

One interesting possibility that has been suggested but never addressed experimentally is the effect of DNA binding on the redox potential of SoxR. The published redox potentials for SoxR were measured in the absence of DNA (19, 22, 23). This is particularly significant because SoxR is activated transcription only in its DNA-bound state, so determining the redox potential of the DNA bound form of SoxR becomes critical.

Given the sensitivity of DNA-modified electrodes in probing redox centers of proteins bound to DNA and the precedent that DNA binding can alter redox potentials of the bound protein, the redox properties of the DNA bound form of SoxR were investigated. Model studies have shown repeatedly the sensitivity of redox potentials of iron-sulfur clusters to environmental perturbations, which are expected to be significant for SoxR (40). Here, using self-assembled DNA monolayers on gold and highly oriented pyrolytic graphite (HOPG), the effect of DNA binding on the redox potential of both *E. coli* and *P. aeruginosa* SoxR was addressed. The potential measured provides convincing evidence for the mechanism the cell uses to maintain SoxR in its reduced form *in vivo*.

RESULTS

Experimental strategy for SoxR electrochemistry on gold

The general strategy for the formation of DNA modified films is shown in Figure 2.1. The electrochemistry of SoxR was first examined on a DNA-modified gold surface. DNA modified with an alkanethiol linker is hybridized with its complement, and assembled onto a gold (1,1,1) on mica surface in a low Mg^{2+} -containing buffer, leading to a loosely packed surface, which leaves room for the protein to bind (9-11). The surface is then backfilled with mercaptohexanol to prevent direct interaction of the protein with the surface (41, 42). DNA-modified gold assemblies were incubated with SoxR at room temperature, then scanned using cyclic and square wave voltammetry. Very small protein-dependent signals were seen with cyclic voltammetry; however, square wave voltammetry revealed a signal from the DNA-bound SoxR. This signal was seen at +40 mV versus NHE (Figure 2.2). These initial studies demonstrated that the oxidation and reduction of the [2Fe2S] clusters in SoxR is possible in a DNA-mediated fashion, and like previous studies on BER enzymes, that DNA binding greatly alters the redox properties of SoxR. In this case, the protein undergoes a positive shift in its redox potential.

Experimental strategy utilized for SoxR electrochemistry

Electrochemistry was done on graphite to further collaborate the results on gold. In addition, SoxR from the bacteria *Pseudomonas aeruginosa* was studied, as it was empirically shown to be a more stable protein than its *E. coli* counterpart. DNA duplexes were prepared by hybridizing pyrene-modified single stranded DNA with its complement (with or without covalently attached Redmond Red). The duplexes were then self assembled on the graphite in the absence of Mg^{2+} to form a loosely packed DNA monolayer, leaving room for SoxR to bind (9-11). The surface backfilling agent in this case was either octane or decane. (41, 42). The electrode was subsequently incubated with protein, and electrochemical experiments were performed before and

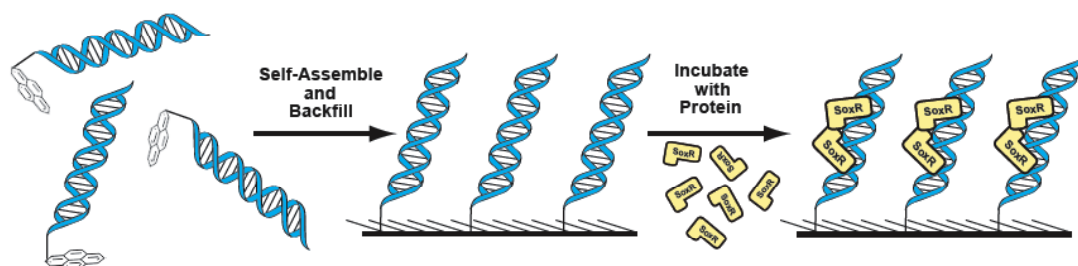


Figure 2.1: Schematic illustration of the self-assembly/backfilling of a DNA monolayer followed by incubation with protein. A strand modified at the 5' end is hybridized with its complement in solution. The double-stranded oligonucleotides are incubated with the electrode surface, and backfilled with an alkane monolayer. The surface is washed, and subsequently incubated with a solution containing protein, which is allowed to bind. In this example, pyrene-modified DNA is put down on a HOPG surface.

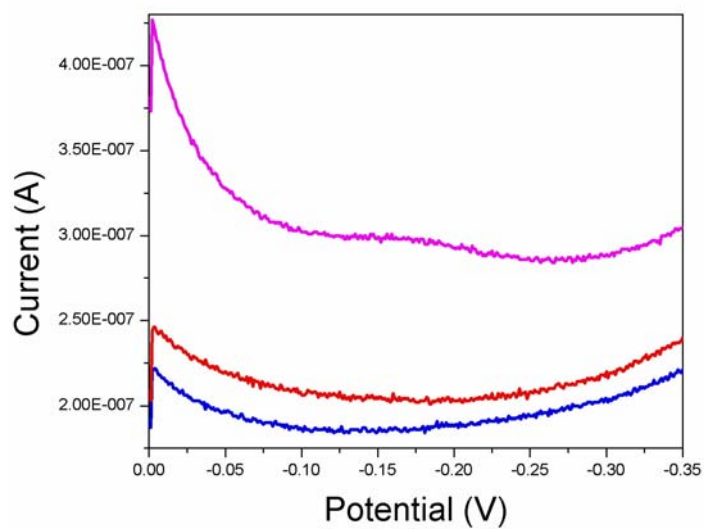


Figure 2.2: Square wave voltammetry at 20 mV/s of Au(1,1,1) on mica electrodes. Red: Voltammogram of DNA in the absence of SoxR. Blue: Voltammogram of DNA incubated with SoxR in a high salt buffer. Magenta: Voltammogram of DNA incubated with SoxR in a low salt buffer. The sequence used in these experiments was 5'-ACCTCAAGTTAACTTGAGGAATT-3' and its complement.

after addition of protein. The DNA binding sites for SoxR are 18 bp symmetrical sequences that are conserved across species (30). For *P. aeruginosa* experiments, the SoxR binding site chosen is found upstream of an operon that encodes the efflux pump MexGHI-OpmD in *P. aeruginosa* PA14.

SoxR binding is reported through the Redmond Red electrochemical signal

Protein binding in electrochemistry experiments can be observed by monitoring the DNA-mediated transport between the electrode and the redox active probe Redmond Red that is attached at either end of the DNA duplex (Figure 2.3). The midpoint potential of Redmond Red is -160 mV vs NHE, and the linearity of the plot of peak current as a function of scan rate indicates that Redmond red behaves as a surface-bound species (43). Although small potential shifts (~20 mV) in the Redmond red signal are occasionally observed upon addition of SoxR, Redmond red provides a convenient and reliable internal standard.

It is expected that a redox-active probe located at the top of the DNA monolayer will report on perturbations of the base pair stack that intervene between the redox probe and the electrode, whereas the same probe located at the bottom of the monolayer near the electrode surface will not be affected by disruptions in base stacking above the probe. Previously, we have reported attenuation of charge accumulation for covalently attached daunomycin due to perturbations of DNA structure by the base-flipping methylase M.HhaI and TATA binding protein (43). When Redmond Red is incorporated above the SoxR binding site, a 16% decrease in the integrated cathodic charge of Redmond Red is observed upon addition of SoxR. In contrast, when Redmond Red is incorporated at the bottom of the DNA duplex below the SoxR binding site, there is little detectable change in the presence of SoxR. Although the loss of signal observed upon addition of SoxR is far smaller than that found for TATA-binding protein or M.HhaI, the decrease in electrochemical signal when the binding site is positioned between the probe and the electrode does provide evidence for proper SoxR binding.

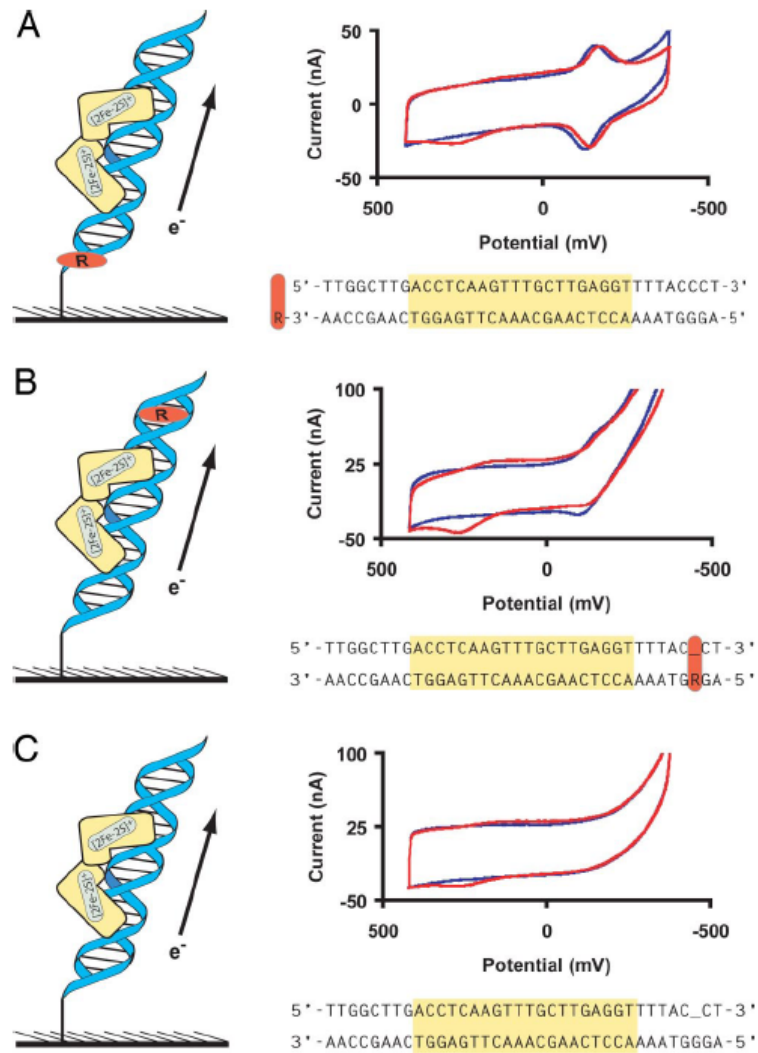


Figure 2.3: Cyclic voltammetry at 50 mV/s of electrodes modified with DNA featuring Redmond Red at the bottom (top), Redmond Red above the binding site (middle), and no Redmond Red (bottom). Voltammograms before addition of SoxR are in blue while ones after addition of SoxR are in red. The sequences used in the course of these experiments are illustrated with the binding sequence for SoxR in red, the location of Redmond Red indicated by an R and the location of abasic sites outlined.

Electrochemistry of P. aeruginosa SoxR

A second distinct and reversible electrochemical signal is observable at +200 mV versus NHE upon addition of SoxR, as evident in Figure 2.3. The signal is observed only after SoxR addition and is not affected by the Redmond Red, as it is also present in the absence of the probe. Note that no redox signature is observed at -290 mV versus NHE, the potential previously reported for SoxR in solution (Figure 2.3). Incubation of the DNA-modified surface with PA2274, a control protein that lacks an iron sulfur cluster, does not result in the appearance of any redox signature. Furthermore, experiments with SoxR stocks featuring low iron sulfur content do not lead to appreciable cyclic voltammetric signals (data not shown). Therefore, we can assign the new signal observed to the [2Fe2S] cluster of SoxR.

In a typical experiment, the observed SoxR signal grows in over a period of 15 minutes and is stable for a minimum of 18 scans before slowly decaying (Figure 2.4), although we have found a high variability in electrode stability upon addition of protein. High concentrations of protein (>10 mM) are required for these experiments, certainly concentrations higher than is required for site-specific binding, and both the high protein concentrations and long DNA sequences used make DNA/protein film formation difficult. It is important to note that the Redmond Red signal is highly stable and exhibits no noticeable degradation during typical electrochemistry experiments.

As can be seen in Figures 2.3 and 2.4, the cathodic and anodic waves observed for SoxR are asymmetric: the oxidation wave is pronounced and substantially less broad compared to the reduction wave. In an ideal quasi-reversible system, the anodic to cathodic peak current ratio is unity (44, 45), but this is certainly not the case for SoxR. We find an anodic to cathodic peak current ratio of 3.0 for SoxR, strongly indicative of a non-ideal and quasi-reversible electrochemical response. In contrast, the anodic to cathodic peak current ratio is 1.3 for Redmond Red on the same film, far closer to the ideal value for a fully reversible system. These

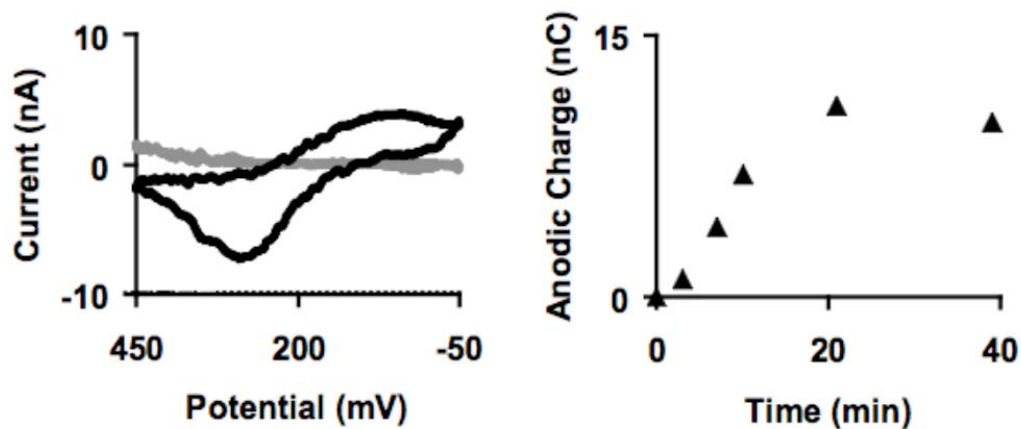


Figure 2.4: Binding of SoxR to the DNA-modified film is shown. Left: Background subtracted cyclic voltammometry of *P. aeruginosa* SoxR at DNA-modified graphite electrodes at a 50 mV/s scan rate immediately after addition of SoxR (light grey) and 20 min after addition of SoxR (black), revealing the signal observed. Right: Integrated anodic charge for SoxR showing the growth of the signal as a function of time.

data strongly indicates that the electrochemistry of SoxR is complicated, hardly surprising given that SoxR binds DNA as a dimer.

Interestingly, the asymmetries in the reduction and oxidation waves of SoxR are qualitatively distinct from those previously observed for the BER enzymes, MutY and Endo III; the electrochemistry of these enzymes featured a reduction wave that was somewhat more pronounced than the oxidation wave (9). The better resolved anodic wave of SoxR integrates to very low surface coverages of 0.5 pmol/cm². This low apparent coverage comparable to that of 2 pmol/cm² previously found for MutY at DNA monolayers on gold (9) and may reflect poor coupling of the iron-sulfur cluster with the base pair stack. However, the Redmond red probe at the bottom of the DNA monolayer integrates to surface coverages of 1 pmol/cm² whereas the Redmond red probe at the top of the film integrates to coverages that are 3-fold lower (over samples sizes of at least 10 electrodes). These values are far less than the ideal DNA surface coverage of 10 pmol/cm² expected for a loosely packed DNA monolayer and indicate that the amount of DNA on the surface is the main determinant of the size of the SoxR signal.

Despite the broad cathodic wave, an upper bound for the number of electrons transferred for the oxidation of SoxR can be calculated. For an ideal surface-bound species, the slope derived from the plot of peak current as a function of scan rate divided by the integrated charge Q at any scan rate is equal to

$$nF / 4RT$$

where F is Faraday's constant, R is the gas constant, and T is the temperature (45); performing this operation for the Redmond red probe at the bottom of the monolayer ($Q_{\text{anodic/cathodic}} \approx 17$ nC at any scan rate) yields a value of $n = 2$, as expected for 2 e⁻ transfer to the resorufin moiety. The integrated charge for the anodic wave of SoxR on the same film varies from 3 to 9 nC, indicating that SoxR receives at most half the number of electrons transferred to the Redmond red. If we assume that all of the DNA is bound and that the Redmond red signal at the bottom of the monolayer corresponds perfectly to the number of DNA molecules on the surface (highly likely

for the sparse films obtained), we can estimate that each DNA-bound SoxR dimer undergoes at most a one electron oxidation/reduction. In fact, all of these observations are consistent with titrations of free SoxR, which deviate from ideal reductions, but appear also to yield values of $n=1$ (23, 46).

Comparison of the voltammetry of E. coli and P. aeruginosa SoxR

E. coli and *P. aeruginosa* SoxR was directly compared to compare the redox chemistry of the protein from multiple organisms. Only weak cyclic voltammetry was observed for *E. coli* SoxR obtained from both the Demple group and Newman group. Therefore, the comparison was made using square wave voltammetry, which is a more sensitive technique and allows for better discrimination of small signals. As can be seen in Figure 2.5, the potentials, references to the Redmond red internal standard, are nearly identical for both *P. aeruginosa* SoxR and *E. coli* SoxR. This observation is consistent with the *in vitro* redox titrations of SoxR that found their potentials to differ by ~ 10 mV (22, 23, 30). In these experiments, the DNA-bound potentials are indistinguishable. The identical redox potentials of the free and DNA bound *E. coli* and *P. aeruginosa* SoxR should allow both to activate transcription upon oxidation, and in fact, previous work has shown that *P. putida* SoxR is functional and can complement an *E. coli* SoxR deletion mutant lending credence to the *in vivo* importance of these observations (28).

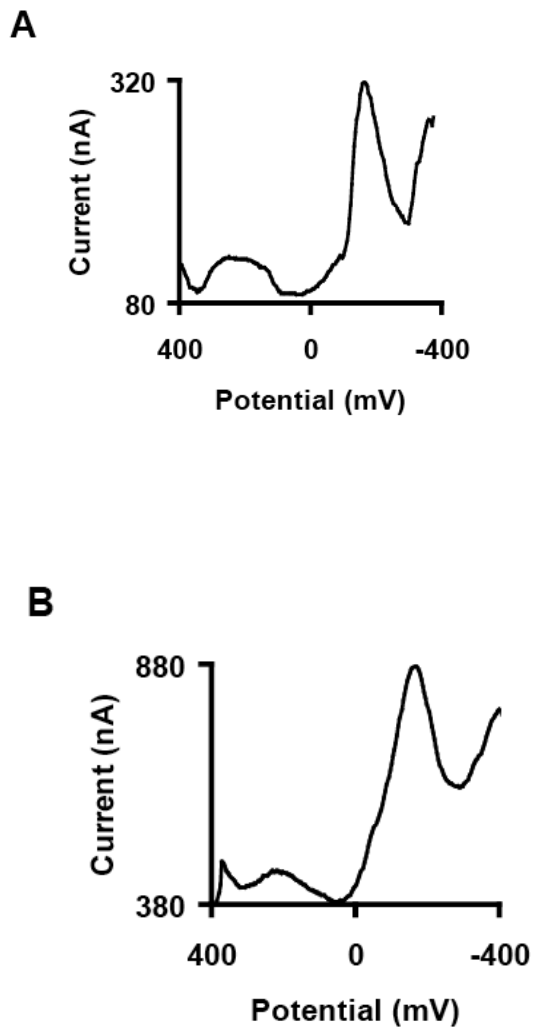


Figure 2.5: Square wave voltammetry of *P. aeruginosa* SoxR (top) and *E. coli* (bottom) at DNA-modified graphite electrodes at a frequency of 15 Hz showing both the Redmond Red and SoxR signals. The 5' Redmond Red-modified sequence was 5'- AGR GTA AAA CCT CAA GCA AAC TTG AGG TCA AGC CAA-3' plus pyrene-modified complement where R indicates the position of the probe.

DISCUSSION

The activity of SoxR, a transcription factor containing an Fe-S cofactor, is regulated via a redox switch: SoxR triggers transcription in its oxidized state but not in its reduced state (19, 20). However, the redox potentials of free *E. coli* and *P. aeruginosa* SoxR have previously been determined to be about -290 mV in solution (22, 23, 30). Although the redox potential of SoxR can explain how it is maintained in its reduced state by coupling it to the cellular NADPH/NADP⁺ pool (-340 mV), it was unclear how the relatively low potential of -290 mV would allow for specificity *in vivo*. To understand the activation of SoxR at a mechanistic level, determining its redox potential within an appropriate context is crucial.

Here, using DNA-modified HOPG electrodes, we have demonstrated that DNA association positively shifts the redox potential of SoxR to 200 mV versus NHE. The +490 mV shift between the free and DNA-bound states of SoxR is functionally crucial, since it keeps SoxR reduced at intracellular potentials, estimated to be -260 to -280 mV in *E. coli* (35). For example, Figure 2.6 shows standard and free midpoint potentials for a variety of cellular redox pairs, and where DNA-bound and free SoxR are positioned along this series. While numerous redox couples, ranging from glutathione to FADH₂, are oxidants for soluble SoxR, they are reductants to DNA-bound SoxR. In fact, the positive shift in potential associated with DNA binding means that DNA-bound SoxR is primarily in the reduced, transcriptionally silent form *in vivo*. Oxidative stress serves to promote oxidation of DNA-bound SoxR, activating the numerous genes required to protect the organism. This provides a rationale for how SoxR can serve as an effective sensor of oxidative stress in *E. coli*.

In *P. aeruginosa*, the paradigm for SoxR activation may be different. Here activation may be promoted by pyocyanin. When we consider the standard potential of the phenazine pyocyanin ($E_m = -34$ mV at pH 7 and $E_m = -110$ mV at pH 8), we predict it would also act as a reductant for DNA-bound SoxR (47). However, pyocyanin is an extracellular electron shuttle that reacts readily with oxygen, as indicated by the bright blue color of *P. aeruginosa* cultures.

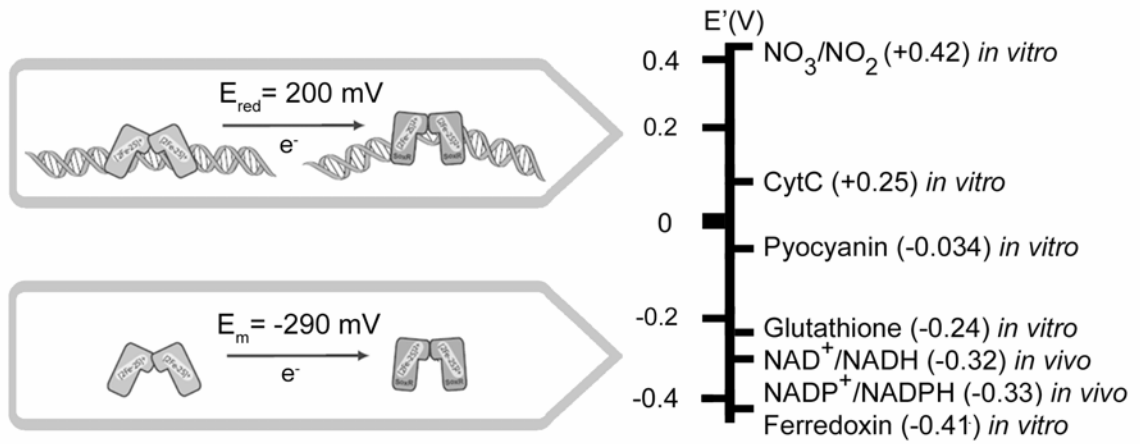


Figure 2.6: Redox potentials of free and DNA-bound SoxR along with those of cellular oxidants/reductants at pH 7.

Uptake of oxidized pyocyanin increases the intracellular ratio of the oxidized versus the reduced form and thus favors the oxidation of SoxR. Considering a one-electron transfer under physiological conditions (pH 7; 37°C), to shift the redox equilibrium of DNA-bound SoxR toward its oxidized state would require a ratio of oxidized to reduced pyocyanin of at least 6500 to 1. Whether this is of physiological relevance in *P. aeruginosa* remains to be determined.

The substantial shift in SoxR potential on DNA binding of ~500 mV is striking but understandable. The significance of the molecular environment for tuning the redox potentials of Fe-S clusters is well documented: each hydrogen bonding interaction with the cluster can cause a potential shift of ~80 mV (46-50). Moreover, for [4Fe-4S] clusters in proteins, all with the same ligating residues, cluster potentials vary from about -600 mV for ferredoxins to about +400 mV for high-potential iron proteins (51). We have previously observed a *negative* shift of at least ~200 mV for Endo III in the presence of DNA (11). Since the structures of Endo III with and without DNA were known and showed no significant distortion in the protein (52-54), thermodynamically this shift was interpreted as a favorable shift in the binding affinity of the protein in the oxidized form relative to the reduced form (11), perhaps not so surprising on binding to the DNA polyanion. In contrast, while the binding affinities of oxidized and reduced SoxR are comparable (21, 22), SoxR and other MerR-type transcriptional regulators have been shown to induce conformational changes of the promoter region (55-60). In particular, copper phenanthroline footprinting studies have provided strong evidence that SoxR significantly distorts its promoter sequence (61, 62). Although this experiment only reports on the reduced form of SoxR, the observed loss of signal for Redmond Red found here strongly supports a DNA distortion mechanism. We propose that the more *positive* reduction potential for DNA-bound SoxR yields a higher energy complex, which may drive a conformational change in the protein/DNA complex. If this were the case, it would constitute an effective means of allosteric regulation *in vivo*. It is important to note that the crystal structure of SoxR in any form has not been solved (63). Therefore, the structural difference between the free (low energy) and DNA-

bound (high energy) complexes is not clear, but a positive shift of the magnitude we observe has been associated with bulk folding of other metalloproteins from *P. aeruginosa* (64). These energetic differences have been attributed to burying the cofactor in a more hydrophobic environment. We predict a similarly large structural difference between the free and DNA-bound SoxR to provide a rationale for the dramatic shift in potential associated with binding.

Within a broader context, these data illustrate that it is critical to take the effect of DNA binding into account when considering the redox characteristics of DNA-binding proteins. It is also likely that it is the DNA-bound potential of these proteins that is most relevant within the crowded environment of the cell, and this potential may be altered even further upon recruitment of RNA polymerase. Therefore, in many cases, as with SoxR, it is perhaps the redox characteristics within a multiprotein/DNA complex that must be considered. In fact, since several transcription factors feature iron sulfur clusters as sensor elements, a change in the redox potential of these cofactors upon binding DNA may generally be an important trait to consider.

EXPERIMENTAL

Materials

All phosphoramidites and reagents for DNA synthesis were purchased from Glen Research. All organic solvents (acetonitrile, dichloromethane, N,N-dimethylformamide) and reagents (1-pyrenebutyric acid, NHS ester) were purchased from Aldrich in the highest available purity and used as received. 1,6-diaminohexane was obtained from Acros Organics.

Oligonucleotide synthesis

Oligonucleotides were prepared using standard phosphoramidite chemistry on an ABI 394 DNA Synthesizer. DNA was purified by HPLC on a reverse phase C18 column with acetonitrile and ammonium acetate as the eluents. The desired products were characterized by high pressure liquid chromatography, UV-visible spectroscopy and MALDI-TOF mass spectrometry.

For the thiol-modified oligonucleotides, DNA was modified with a free thiol at the 5' terminus as previously described (2, 3). The strand of interest was synthesized (see above) using manual cleavage from the CPG resin without the trityl group. The sequence of this strand is as follows: 5'-ACCTCAAGTTAACTTGAGGAATT-3'. The 5' phosphate group of the DNA was activated using carbonyl diimidazole in acetonitrile (CDI, Sigma) and shaking for one hour, after which the hexamine diamine (Acros) linker in acetonitrile was added and was allowed to react with shaking for 25 min. The DNA was then filtered through a NAP-10 column. DNA was then cleaved from the resin with concentrated NH₄OH for one hour, spin dried, and reconstituted in 200 mM HEPES pH 8.0. A thiol group was added using N-Succinimidyl 3-[2-pyridyldithio]-propionamido (SPDP, Pierce) in MeCN, and was allowed to react with shaking for 45 min. The reaction was quenched in phosphate buffer and the aqueous layer was eluted through a NAP-5 column. The strand was purified via HPLC, lyophilized, and resuspended in phosphate buffer. The thiol-protecting group was removed with dithiothreitol (DTT, Aldrich) with shaking for one

hour and SH-DNA was then purified again via HPLC, lyophilized, and reconstituted in 50 mM phosphate buffer, and purified via ethanol precipitation.

For experiments on HOPG, DNA was modified with pyrene at the 5' terminus by following a previously reported procedure (4). In brief, oligonucleotides were prepared by solid phase synthesis using standard reagents with an unprotected hydroxyl group at the 5' terminus. The 5'-OH was treated with a 120 mg/mL solution of carbonyldiimidazole in dioxane for 2 hours followed by an 80 mg/mL solution of 1,6-diaminohexane for 30 min. Subsequently, the free amine was treated with 1-pyrenebutyric acid, N-hydroxysuccinimide ester, resulting in the desired pyrene moiety linked to the 5' terminus. The oligonucleotides were deprotected with concentrated NH_4OH at 60°C for 8 hours.

DNA modified with Redmond Red at the 3' terminus or 3 bases in from the 5' terminus was prepared according to the ultramild protocols outlined on the Glen Research website (www.glenres.com). Pac protected bases and ultramild reagents were used during the course of the solid phase synthesis to prevent undesirable capping of the protecting groups. The oligonucleotides were deprotected in 0.05 M potassium carbonate in methanol at room temperature for 12-14 hours to prevent degradation of the Redmond Red moiety under harsh conditions.

Expression and purification

E. coli SoxR was prepared as previously described (65). N-terminally histidine-tagged SoxR from *P. aeruginosa* PA14 were expressed from plasmid pET16b in *Escherichia coli* strain BL21 (DE3). For this, cells were grown in 1L LB medium with 100 $\mu\text{g}/\text{mL}$ ampicillin at 37°C. At an $\text{OD}_{600\text{nm}}$ of 0.3 protein expression was induced by the addition of 1 mM IPTG and the cultures were incubated for an additional ten hours at 16°C. All following steps were performed at 4°C. Cells were pelleted, resuspended in buffer A (50 mM NaH_2PO_4 , pH 8.0, 300 mM NaCl,

10% glycerol) containing 10 mM imidazole and PIC (protease inhibitor cocktail without EDTA; Roche) and lysed using a French Press. The cell extract was centrifuged at 14,000 g for 20 min. The supernatant was incubated with Talon beads for 30 min then transferred to a column. The beads were washed with buffer A containing 50 mM imidazole and PIC. Histidine tagged SoxR was eluted from the column with buffer A containing 250 mM imidazole and PIC. Peak fractions and purity were determined by running an SDS-PAGE followed by Coomassie Blue staining. Purified protein was dialyzed against buffer A.

To generate expression plasmid pET16b-soxR, *soxR* (PA14_35170) was PCR amplified from genomic DNA of *Pseudomonas aeruginosa* PA14 using primers A (CGC catatg AAG AAT TCC TGC GCA TC) and B (GGC gga tcc CTA GCC GTC GTG CTC G). Primer A contains an NdeI restriction site (small letters) and *soxR*'s start codon (underlined). Primer B contains a BamHI site (small letters) and *soxR*'s stop codon. The PCR fragment was ligated into NdeI/BamHI-digested pET16b.

Formation of DNA monolayers and electrochemical measurements

For experiments on gold, 100 μ M of thiolated DNA was annealed with its complement, then was added to a gold (111) on mica surface for 24 hrs to form a loosely packed film. The surface was then backfilled with mercaptohexanol. Pt wire served as the auxiliary electrode and the reference electrode was Ag/AgCl with modified tip containing 4% agarose in 3 M NaCl. Cyclic voltammetry (data not shown) and square wave voltammetry were performed on a CHI760B electrochemical workstation. Scan rate used was 0.02 V/s.

For experiments on graphite, DNA films were self-assembled on SPI-1 grade HOPG electrodes (SPI) with an estimated surface area of 0.08 cm² defined by an o-ring. Duplex DNA was formed in pH = 8, 50 mM P_i, 500 mM NaCl, 20% glycerol buffer (SoxR storage buffer) by combining equimolar amounts of the pyrene-modified strand with its complement. Loosely packed DNA monolayers were allowed to form over a period of 24-48 hours. Subsequently, the

electrodes were thoroughly rinsed with SoxR storage buffer before being backfilled for 2-4 hours with 10% by volume octane or decane solutions in SoxR dialysis buffer. The electrodes were thoroughly rinsed with SoxR storage buffer again to eliminate residual octane/decane and moved into a nitrogen atmosphere for electrochemistry experiments.

Electrochemical data were collected using a Bioanalytical Systems CV-50W potentiostat using the inverted drop cell configuration. All measurements reported for the working electrode were taken vs. a platinum (Pt) auxiliary and a silver/silver chloride (Ag/AgCl) reference. The Ag/AgCl reference was frequently standardized vs. SCE, and all reported potentials have an experimental uncertainty of less than 40 mV. Electrochemical experiments were performed at ambient temperature and under an anaerobic atmosphere in SoxR storage buffer. In a typical experiment, background electrochemical scans were performed before SoxR was added to the storage buffer, resulting in a ~15-35 μM monomer concentration within the cell. Further scans were then performed in the presence of SoxR, typically over a period of thirty to forty five minutes.

REFERENCES

1. Gorodetsky, A.A., Buzzeo, M.C., Barton, J.K. *Bioconj. Chem.* 19:2285-2296 (2008).
2. Kelley, S.O., et al. *Nucleic Acids Res.* 27:4830-4837 (1999).
3. Boon, E.M. et al. *Nat Biotechnol* 18:1096-1100 (2000).
4. Gorodetsky, A.A., Barton, J.K. *Langmuir* 22:7917-7922 (2000).
5. Kelley, S.O., Jackson, N.M., Hill, M.G., Barton, J.K. *Angew. Chem. Int. Ed.* 38:941-945 (1999).
6. Inouye, M., et al. *Proc. Natl. Acad. Sci. USA* 102:11606-11610 (2005).
7. Okamoto, A., Kamei, T., Saito, I. *J. Am. Chem. Soc.* 128:658-662 (2006).
8. Gorodetsky, A.A., Green, O., Yavin, E., Barton, J.K. *Bioconjugate Chem.* 18:1434-1441 (2007).
9. Boon, E.M., et al. *Proc. Natl. Acad. Sci. USA* 100:12543-12547 (2003).
10. Boal, A.K. et al. *Biochemistry* 44:8397-8407 (2005).
11. Gorodetsky, A.A., Boal, A.K., Barton, J.K. *Biochemistry* 44:8397-8407 (2005).
12. Cunningham, R.P., et al. *Biochemistry* 28:4450-4455 (1989).
13. Asahara, H. et al. *Biochemistry* 28:4444-4449 (1989).
14. Fu, W. et al. *J. Biol. Chem.* 267:16135-16137 (1992).
15. Boal, A.K., Yavin, E., Barton, J.K. *J. Inorg. Biochem.* 101:1913-1921 (2007).
16. Brown, N.L., Stoyanov, J.V., Kidd, S.P., Hobman, J.L. *FEMS Microbiol. Rev.* 27:145-163 (2003).
17. Hobman, J.L., Wilkie, J., Brown, N.L. *Biometals* 18:429-436 (2005).
18. Giedroc, D.P., Arunkumar, A.I. *J. Chem. Soc. Dalton Trans.* 3107-3120 (2007).
19. Pomposiello, P.J., Demple, B. *Trends Biotechnol.* 19:109-114 (2001).
20. Demple, B., Ding, H., Jorgensen, M. *Methods Enzymol* 348:355-364 (2002).
21. Hidalgo, E., Demple, B. *EMBO J.* 13:138-146 (1994).
22. Gaudu, P., Weiss, B. *Proc. Natl. Acad. Sci. USA* 93:10094-10098 (1996).

23. Ding, H., Hidalgo, E., Demple, B. *J. Biol. Chem.* 271:33173-33175 (1996).
24. Ding, H., Demple, B. *Proc. Natl. Acad. Sci. USA* 94:844508449 (1997).
25. Pomposiello, J., Bennik, M.H.J., Demple, B. *J. Bacteriol* 183:3890-3902 (2001).
26. Ha, U., Jin, S. *Infect. Immun.* 67:5324-5331 (1999).
27. Stover, C.K. et al. *Nature* 406:959-964 (2000).
28. Park, W., Pena-Llopis, S., Lee, Y., Demple, B. *Biochem. Biophys. Rev. Commun.* 341:51-56 (2006).
29. Dietrich, L.E.P., et al. *Mol. Microbiol.* 61:1308-1321 (2006).
30. Kobayashi, K., Tagawa, S. *J. Biochem.* 136:607-615 (2004).
31. Zheng, M., Storz, G. *Biochem. Pharmacol.* 59:1-6 (2000).
32. Liochev, S.I., Fridovich, I. *Proc. Natl. Acad. Sci. USA* 89:5892-5896 (1992).
33. Kobayashi, K., Tagawa, S. *FEBS Lett.* 451:227-230 (1999).
34. Koo, M-S., et al. *EMBO J.* 22:2614-2622 (2003).
35. Hwang, C., Lodish, H.F., Sinskey, A.J. *Methods Enzymol.* 252:212-221 (1995).
36. Kobayashi, K., Tagawa, S. *J. Inorg. Biochem.* 67:258 (1997).
37. Liochev, S.I., Benov, L., Touati, D., Fridovich, I. *J. Biol. Chem.* 274:9479-9481 (1999).
38. Ding, H., Demple, B. *Biochemistry* 37:17280-17286 (1998).
39. Price-Whelan, A., Dietrich, L.E.P., Newman, D.K. *J. Bacteriol.* 189:6372-8381 (2007).
40. Stephens, P.J., Jollie, D.R., Warshe, A. *Chem. Rev.* 96:2491-2513 (1996).
41. Kim, Y., Long, E.C., Barton, J.K., Lieber, C.M., *Langmuir* 8:496-500 (1992).
42. Giancarlo, L.C., Flynn, G.W. *Annu. Rev. Phys. Chem.* 49:297-336 (1998).
43. Bard, A.J., Faulkner, L.R. *Electrochemical Methods* (New York: Wiley), 2nd edition (2001).
44. Boon, E.M., Salas, J.E., Barton, J.K. *Nat. Biotechnol.* 20:282-286 (2002).
45. Udit, A.K., et al. *J. Am. Chem. Soc.* 126:10218-10219 (2004).
46. Hidalgo, E., Ding, H., Demple, B. *Trends Biochem.* 22:207-210 (1997).

47. Price-Whelan, A., Dietrich, L.E.P., Newman, D. *Nat. Chem. Biol.* 2:71-78 (2006).
48. Rusling, J.F. *Acc. Chem. Res.* 31:363-369 (1998).
49. Carter, C.W., Jr., et al. *Proc. Natl. Acad. Sci. USA* 69:3526-3529 (1972).
50. Heering, H.A., Bultink, Y.B.M., Hagen, W.E., Meyer, T.E. *Biochemistry* 34:14675-14686 (1995).
51. Beinert, H. *J. Biol. Inorg. Chem.* 5:2-15 (2000).
52. Kuo, C.F. et al. *Science* 258:434-440 (1992).
53. Thayer, M.M. et al. *EMBO J.* 14:4108-4120 (1995).
54. Fromme, J.C., Verdine, G.L. *EMBO J.* 22:3461-3471 (2003).
55. Ansari, A.Z., Bradner, J.E., O'Halloran, T.V. *Nature* 374:371-375 (1995).
56. Outten, C.E., Outten, F.W., O'Halloran, T.V. *J. Biol. Chem.* 274:37517-37524 (1999).
57. Zheleznova-Heldwein, E.E, Brennan, R.G. *Nature* 409:378-382 (2001).
58. Godsey, M.H., et al. *J. Biol. Chem.* 276:47178-47184 (2001).
59. Changela, A. et al. *Science* 301:1383-1387 (2003).
60. Newberry, K.J., Brennan, R.G. *J. Biol. Chem.* 279-20356:20362 (2004).
61. Hidalgo, E., et al. *J. Biol. Chem.* 270:28908-28914 (1995).
62. Hidalgo, E., Demple, B. *EMBO J.* 16:1056-1065 (1997).
63. Watanabe, S., et al. *Act. Crystallogr. F.* 62:1275-1277 (2006).
64. Wittung-Stafshede, P., et al. *J. Biol. Inorg. Chem.* 3:367-370 (1998).
65. Chander, M., Demple, B. *J. Biol. Chem.* 279-41603-41610 (2004).

Chapter 3

Effects of SoxR on the Formation of Guanine Radical Induced Damage to DNA

INTRODUCTION

Oxidative damage in cells

Oxidative insults to the DNA of a cell start as oxidative radicals. In nature, these radicals are often formed when a reactive oxygen species (ROS), often the hydroxyl radical ($\text{OH}\cdot$), interacts with the base stack of DNA; this accounts for over half of all the oxidative damage that can occur in DNA; the remainder are reactions at deoxyribose that can lead to abasic sites or strand breaks (1). The reactions of $\text{OH}\cdot$ with the DNA bases have been reviewed (2, 3) and involve the addition of $\text{OH}\cdot$ to the C5 position of pyrimidines and the C4, C5, or C8 position of purines, followed by dehydration. In the case of guanine, this dehydration is coupled to transfer of a proton across the hydrogen bond from cytosine to form the neutral guanine radical ($\text{G}(-\text{H})\cdot$). This oxidative radical, or hole, is relatively long lived in DNA, having a half-life in the millisecond timescale (4).

In the laboratory, guanine radicals can be generated in DNA using a variety of organic or inorganic photooxidants. The most commonly used organic photooxidant is anthroquinone; in contrast, there are a wide variety of inorganic photooxidants based off of second- and third-row transition metals, i.e., Ru, Rh, Os, Ir, and Re. These complexes typically contain an intercalating ligand, such as dipyridophenazine (dppz) or phenanthrenequinone diimine (phi), which is able to fit between two adjacent bases in the DNA base stack, and two ancillary ligands that may determine the redox properties of the complex, or provide additional functionality, such as a handle for covalently tethering the complex to the DNA backbone (5). Intercalation improves the affinity of these complexes for DNA, which in turn facilitates their ability to inject holes into the π -stack of the bases.

Ruthenium chemistry

Tris-heteroleptic complexes of Ru, in particular $[\text{Ru}(\text{phen})_2\text{dppz}]^{2+}$ and $[\text{Ru}(\text{phen})(\text{dppz})(\text{bpy})]^{2+}$ are luminescent in the presence of non-polar solvents when irradiated at

442 nm, which promotes an electron into a MLCT band from the Ru d-orbital to a π^* orbital on the dppz or bpy ligand. This state is emissive, except for in polar solvents, where hydrogen bonding to phenazine nitrogens of the dppz ligand causes the electron to undergo rapid radiationless decay, quenching luminescence. However, when the dppz ligand is intercalated into DNA, these nitrogens are protected from quenching, causing complexes to act as light switches for DNA (6).

The long luminescent lifetimes for the Ru complexes also allow them to participate in flash-quench mechanisms (Figure 3.1). In this reaction, the complex is irradiated, promoting an electron into an excited state. An external electron acceptor can act as a quencher of this luminescent state, leaving the metal in a higher valence oxidation state, Ru(III). This quenching occurs very fast, along the order of hundreds of nanoseconds (4). The species that is formed is a powerful ground state oxidant (1.60 V vs NHE), which can inject a hole into DNA (7), abstracting electrons from sites with low oxidation potentials, i.e., guanines (1.29 V vs NHE) or guanine doublets (8, 9).

If these transient base radicals are allowed to react with water or oxygen, they lead to persistent guanine oxidation products, notably 8-oxo-guanosine, which is also a biologically relevant DNA damage species. Formation and localization of 8-oxo-guanosine can be monitored by treatment with piperidine, which causes a strand break at the site of oxidation, followed by gel electrophoresis. Importantly, any species that competes with guanine for the hole will attenuate the observed amount of guanine oxidation product in the DNA; this may be accomplished by low potential DNA bound species such proteins with redox-active moieties that are able to access the base stack electronically (10).

The flash quench technique is particularly useful due to the formation of a long-lived ground state, which leads to high quantum yield of hole injection. Oxidation of guanine residues distal to the site of hole injection has been studied using this method with complexes which are covalently tethered to DNA. The ability of holes to transverse the π -stack of DNA has been well

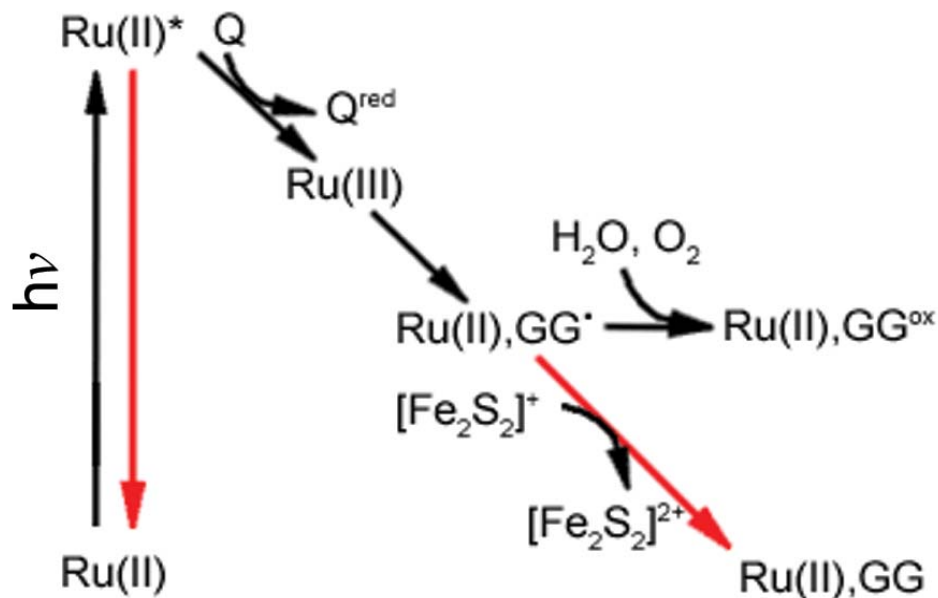


Figure 3.1: The Ru flash quench scheme is shown here. Ground state Ru(II) bound to DNA is irradiated at 442 nm to form excited Ru(II)*. The excited state is quenched by $[Co(NH_3)_5Cl]^{2+}$ or $[Ru(NH_3)_6Cl]^{2+}$ (Q), resulting in Ru(III) in situ, a ground state oxidant able to abstract an electron from guanine doublets in DNA. If the resulting guanine radical is allowed to react with water, permanent damage products, such as 8-oxo-guanine, to form (black arrows). Pathways that prevent formation of damage (red arrows) are recombination processes. If a reduced $[2Fe_2S]^{+}$ cluster from SoxR, bound to DNA, is able to donate an electron becoming the oxidized $[2Fe_2S]^{2+}$ form in the process, permanent guanine damage products are not seen.

documented, in some cases through distances of up to 200 Å (10, 11, 12).

Importantly, the yield of hole injection (and subsequent damage) is affected by several conditions, most importantly, salt concentration, and quencher identity. Two commonly used quenchers are $[\text{Co}(\text{NH}_3)_5\text{Cl}]^{3+}$ and $[\text{Ru}(\text{NH}_3)_6]^{3+}$. The latter has a high efficiency of quenching with the photooxidant, leading to high yields of hole injection; however, rapid back electron transfer decreases the overall yields of damage. On the other hand, $[\text{Co}(\text{NH}_3)_5\text{Cl}]^{3+}$ is less effective as a quencher, but is unstable upon reduction, which eliminates the possibility of back electron transfer to the photooxidant (4), and increases the yield of DNA damage.

The role of guanine radicals in SoxR activation

Given the response of SoxR to species that give rise to oxidative radicals in DNA, and the migratory nature of these radicals, a plausible route for protein oxidation might arise in a DNA-mediated reaction. Under oxidative stress, reactive oxygen species are generated in the cell that, either directly or indirectly as with the superoxide radical (13), promote reactions that oxidatively damage DNA. The formation of guanine radicals can serve as an early signal of oxidative stress within the cell; a generated hole could migrate and rapidly equilibrate at guanine sites of low oxidation potential. A one-electron SoxR oxidation by the guanine radical could both activate transcription factors that respond to oxidative stress and directly repair the base radical. The oxidation of DNA-bound proteins from a distance through DNA charge transport has been established for MutY (14), a base excision repair protein in *Escherichia coli*, and for p53 (15), a mammalian regulator of the cellular response to genotoxic stress.

RESULTS

Flash quench damage to DNA

In order to determine conditions that would lead to high yields of damage to DNA, two different photooxidants and two different quenchers were compared. DNA which was [³²P]-labeled and containing the SoxR binding site in the sequence as well as guanine multiplet sites was incubated with photooxidant and quencher and irradiated. The DNA was treated with piperidine, which cleaved it at sites where base oxidation occurred. The control sample irradiated in the presence of photooxidant, but lacking quencher (LC), and the control sample containing photooxidant and quencher, but which was not irradiated (DC), both show an absence of damage. When both photooxidant and quencher are present and the sample is irradiated, damage is seen localized at guanine residues. When comparing photooxidants, [Ru(phen)(dppz)(bpy)]²⁺ and [Ru(phen)₂dppz]²⁺ (dppz = dipyridophenazine), showed similar yields of damage; however, damage was higher when the sacrificial quencher [Co(NH₃)₅Cl]³⁺ was used versus [Ru(NH₃)₆]³⁺. Importantly, this chemistry does not yield reactive oxygen species such as hydroxyl radicals, and quenching of the excited state of Ru(II) in this manner prevents the sensitization of singlet oxygen (¹O₂) (4).

Since SoxR is stored in a high salt buffer, one concern was that addition of SoxR would decrease the yield of quenching as it would increase the ionic strength of the solution. To determine the dependence of damage yield on salt concentration, a series of steady state fluorescent measurements were performed using [Ru(phen)(dppz)(bpy')]²⁺ as the photooxidant and [Co(NH₃)₅Cl]³⁺. At salt concentrations up to 400 μM, quenching had a fairly linear salt dependence; at salt concentrations of 382 mM, 10 mM [Co(NH₃)₅Cl]³⁺ was required to effectively quench fluorescence of the [Ru(phen)(dppz)(bpy')].

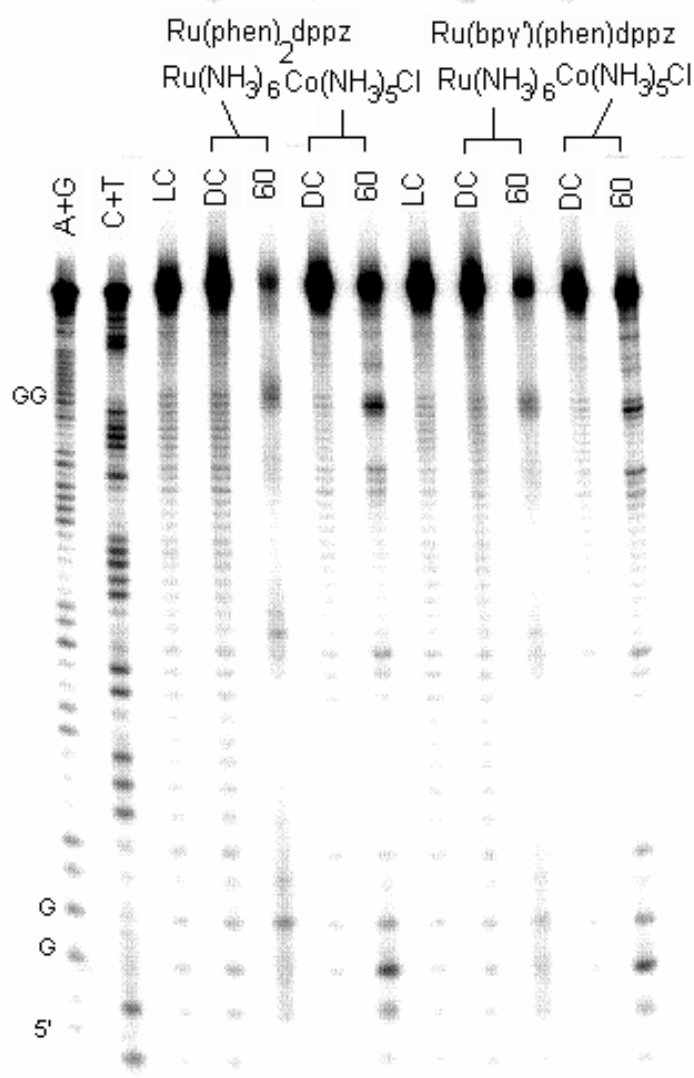


Figure 3.2: A comparison is shown between two different photooxidants and two different quenchers. No damage is seen with photooxidant in the absence of light (DC) or light in the absence of photooxidant (LC). When samples are irradiated in the presence of photooxidant and quencher, damage is seen, specifically at guanine sites and the 5' guanine of guanine doublets. Slightly higher damage is seen using $[\text{Ru}(\text{phen})_2\text{dppz}]^{2+}$ as the photooxidant than with the $[\text{Ru}(\text{phen})(\text{dppz})(\text{bpy}')]$. This may be due to the fact that the bpy' would cause the latter complex to not bind DNA as avidly as the bisphenanthroline Ru complex. Much higher damage is seen when the sacrificial quencher $[\text{Co}(\text{NH}_3)_5\text{Cl}]^{2+}$ is used versus $[\text{Ru}(\text{NH}_3)_6]^{2+}$, as the sacrificial quencher prevents back-electron transfer from occurring.

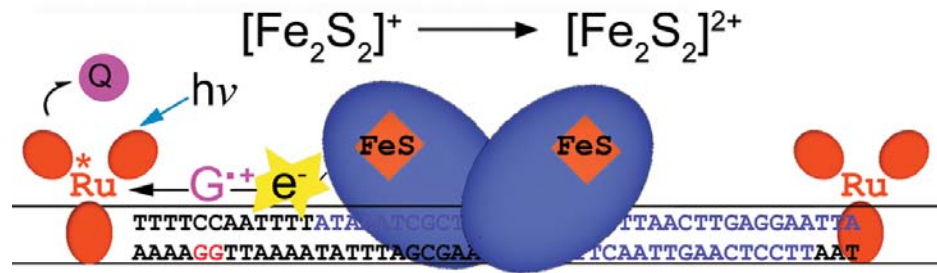


Figure 3.3: The experimental system is shown schematically. SoxR (blue) is bound to its promoter site on DNA. $[\text{Ru}(\text{phen})(\text{dppz})(\text{bpy}')^{2+}]^{2+}$ (red), noncovalently intercalated into DNA, is able to oxidize a guanine residue, and the $[\text{2Fe}_2\text{S}]^+$ cluster of SoxR can donate an electron to fill the resulting hole.

Damage attenuation with SoxR

Guanine radicals persist in DNA for milliseconds before being trapped. Reduced SoxR bound to DNA should therefore be able to compete with guanine residues for these resulting holes. To examine this, holes were generated in DNA using the flash-quench method outlined previously, in the presence or absence of reduced SoxR. Figure 3.3 shows the results of this experiment. Guanine damage is seen in the presence of photooxidant and quencher at guanine residues. In the presence of increasing amounts of SoxR, this damage is attenuated.

Other explanations for the attenuation of guanine damage is that the SoxR is competing for binding of the photooxidant to the DNA, or the low observed yield of damage at high salt concentrations. To distinguish between a redox mechanism, competitive binding, and ineffective quenching, guanine damage was examined in the presence of reduced SoxR versus oxidized SoxR. Since SoxR is bound to DNA in both samples, in its own buffer, the only difference between the samples would be the oxidation state of the protein.

Figure 3.4 shows the results of this experiment testing whether reduced SoxR can inhibit guanine damage. DNA damage is generated at guanine doublets, sites in DNA that are most readily oxidized (16), on a DNA duplex using non-covalently bound $[\text{Ru}(\text{phen})(\text{dppz})(\text{bpy}')]^{3+}$ ($\text{bpy}' = 4\text{-butyric acid } 4'\text{-methyl bipyridine}$). Oxidative damage is evident only in the presence of DNA-bound Ru, quencher and light, and is absent in samples lacking Ru (light control, LC) or samples containing Ru but not irradiated (dark control, DC). Most interesting is the comparison of damage patterns in the presence of SoxR in different oxidation states. When the DNA is irradiated in the presence of SoxR that has been reduced with sodium dithionite, a large attenuation of the damage at guanine residues is observed, indicating that SoxR is able to reduce the guanine radicals and inhibit irreversible damage. This attenuation increases with increased stoichiometric ratios of SoxR to DNA. However, when the DNA is irradiated in the presence of oxidized SoxR, this attenuation in damage is not observed; oxidized SoxR cannot fill the electron hole in the guanine radical. As a control, DNA is irradiated also in the presence of dithionite used

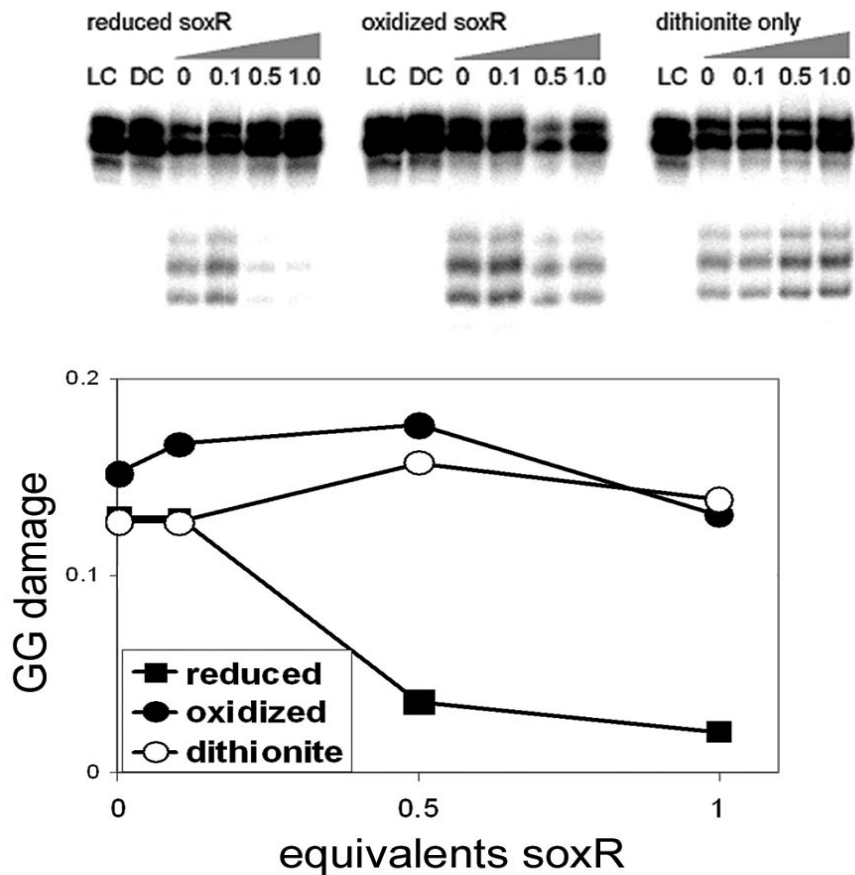


Figure 3.4: Top: Denaturing PAGE analysis of guanine oxidation is shown. A 5'-labeled 48-mer DNA duplex containing the SoxR binding site is irradiated in the presence of photooxidant, quencher, and either reduced SoxR, oxidized SoxR, or an equivalent amount of dithionite as is used to reduce SoxR. Bands corresponding to guanine residues indicate guanine piperidine-labile guanine oxidation has occurred. Bottom: An ImageQuant analysis of the previous gel.

to reduce the SoxR; without SoxR, these samples show no attenuation of damage, indicating that it is not the presence of the reductant in solution that is responsible for the attenuation of guanine damage.

At higher ratios of SoxR:DNA, however, the reduction of damage at guanines diminishes. As shown in Figure 3.5, at a 1:1 ratio of SoxR to DNA, damage at guanine residues is highest for oxidized SoxR, followed by dithionite only, with the least damage being seen in the presence of reduced SoxR. However, at higher ratios of SoxR:DNA, this effect diminishes, and the reduction of damage at guanines is the same whether reduced SoxR, or an equivalent amount of dithionite, is present in the sample. This may be due to the fact that the DNA is saturated with SoxR at ratios above 1:1; any additional unbound reduced SoxR will not have an effect. Instead, dithionite may be attenuating guanine damage directly by reducing the guanine radicals, or indirectly by interfering with quenching of the photooxidant. Indeed, the high binding affinity of SoxR for its promoter site would prevent equilibration of bound oxidized SoxR with reduced SoxR in solution which could accept more holes. An excess of dithionite is commonly used to reduce SoxR, and high total amounts of dithionite in solution will obscure the effect due to reduced SoxR, and may explain the small difference between the dithionite and reduced SoxR containing sample at 1:1 ratios in this experiment.

These results indicate that the [2Fe2S] clusters in SoxR electronically access the DNA base stack and repair oxidative radical damage at guanine sites in DNA. Since SoxR is a redox sensor involved in mediation of oxidative damage in cells, the ability of SoxR to sense radicals in DNA suggests that guanine damage in DNA could be an initial trigger that allows SoxR to detect and respond to harmful oxidizing conditions in the genome.

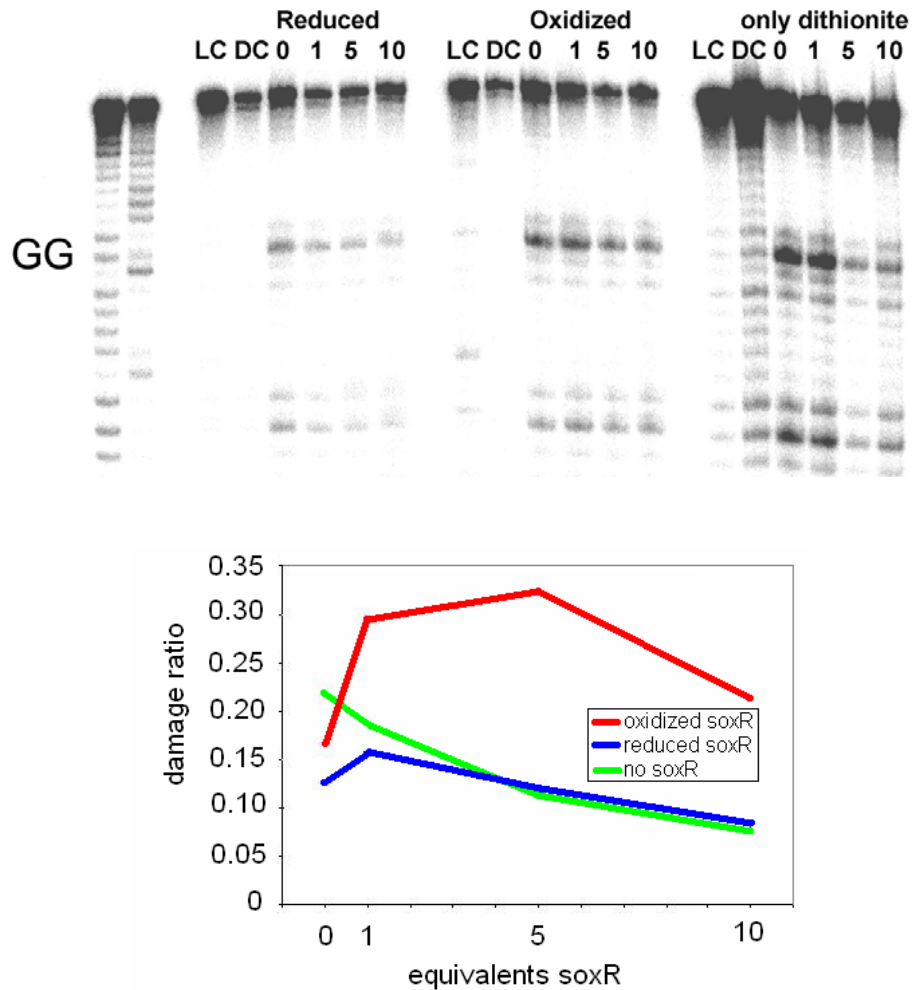


Figure 3.5: Top: PAGE gel analysis of guanine damage in the presence of greater than 1:1 equivalents of SoxR:DNA. Bottom: Quantization of the bands in the gel picture. In the absence of SoxR, no clear trend is seen in the damage patterns. At 1:1 SoxR:DNA ratios, samples containing reduced SoxR show the least damage, followed by samples containing just dithionite, and samples containing oxidized SoxR show the highest amount of damage. However, as SoxR (or the equivalent amounts of dithionite) are added, there is no difference in attenuation between reduced SoxR containing samples and samples containing reductant.

DISCUSSION

SoxR is well established as a sensitive transcriptional regulator that responds to conditions of superoxide ($O_2^{\cdot-}$) stress in *E. coli* and other bacteria. SoxR is able to activate transcription of its target gene by oxidation of one of its $[2Fe_2S]^{+}$ clusters. However, to date, the oxidant for the protein has not been identified. It is unlikely that $O_2^{\cdot-}$ itself is the culprit for oxidizing SoxR, first because $O_2^{\cdot-}$ is a diffusible species whereas SoxR likely remains tightly associated with DNA at its binding site, and secondly, because $O_2^{\cdot-}$ reacts avidly and irreversibly with iron-sulfur clusters of many proteins.

However, it is important to recognize that $O_2^{\cdot-}$ itself is of limited reactivity, whereas its daughter species H_2O_2 and OH^{\cdot} , which arise from reactions with Fe^{3+} via the Fenton reaction, are highly reactive molecules. DNA, in particular, is an important target for attack by these ROSs, due both to the high reactivity of the electron-rich bases and the crucial role this biomolecule plays in the survival of the all organisms. The initial species formed in reactions involving DNA and ROSs is a long-lived base radical, which is able to migrate through the DNA base stack and localize at guanine residues (3).

The purpose of these experiments was to investigate whether these guanine radicals could be reduced by SoxR, thus serving as the signal for SoxR activation. SoxR contains two $[2Fe_2S]^{1+/2+}$ clusters, one of which, when oxidized, causes the protein to act as a transcriptional activator. The relevant $1+/2+$ redox couple of the $[2Fe_2S]$ clusters of DNA-bound SoxR occurs at +200 mV vs NHE (17), which rules out oxidation of the protein by normal cellular oxidants, but is still able to easily reduce guanine radicals in DNA.

Guanine radicals in DNA can be generated efficiently using ruthenium chemistry in a flash-quench scheme (Figure 3.2) (4). In this scheme, oxidative quenching of $[Ru(phen)(dppz)(bpy^{\prime})]^{2+}$ an avid DNA intercalator, yields a ground state Ru(III) *in situ* that oxidizes guanine doublets in DNA, generating guanine radicals and consequently a high yield of irreversible guanine damage (4, 10). $[Co(NH_3)_5Cl]^{2+}$ is utilized as a sacrificial excited state

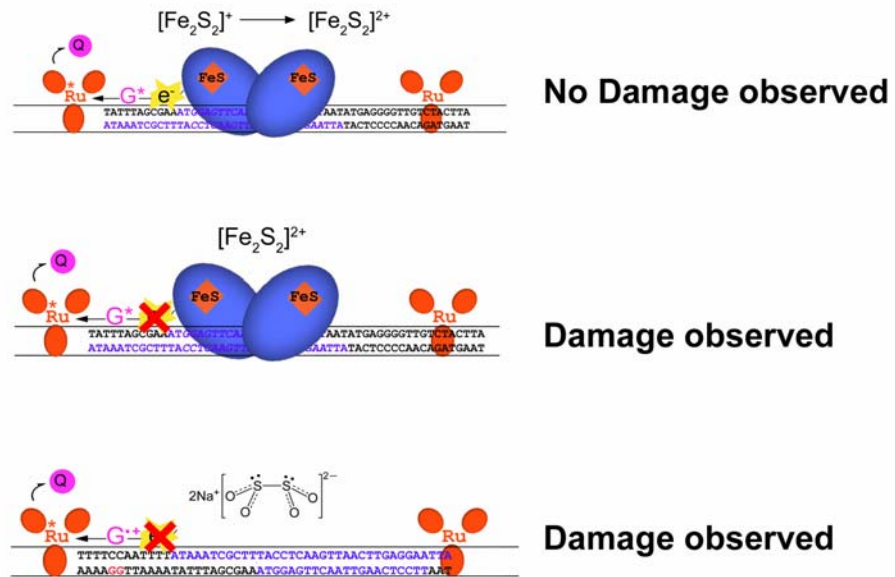


Figure 3.6: A schematic of the guanine oxidation attenuation results. Top: In the presence of reduced SoxR, the hole on guanine is filled by an electron from SoxR, and no damage is observed. Middle: If oxidized SoxR is present in the sample, an electron cannot be donated to fill the hole on the guanine, and damage is observed. Bottom: Dithionite alone cannot reduce the guanine radical directly, and guanine damage is observed.

quencher as it precludes back electron transfer, allowing a high yield of damage to be obtained. Oxidation of a DNA-bound protein can be accomplished by the guanine radicals in order to intercept irreversible guanine damage. This inhibition of guanine damage has been previously demonstrated using DNA-bound MutY (14).

The results of the guanine attenuation experiments with SoxR indicates that this protein can too be oxidized in a DNA-dependent manner. Damage at guanine sites is attenuated by reduced SoxR, which is able to donate an electron through the DNA base stack to pair with the oxidative radical formed through flash quench chemistry (Figure 3.6). Oxidized SoxR, however, can not easily donate an additional electron, and the radicals formed at guanine sites remain, where they eventually become damage products which are visible on the gels. Importantly, this attenuation of damage is not seen in the control sample lacking SoxR, but containing dithionite, which is used to reduce the protein. Furthermore, damage decreases as increasing ratios of SoxR:DNA are examined, but only up to a point; for ratios of SoxR:DNA greater than 1:1, attenuation of damage at guanine sites is indistinguishable from that due to dithionite only. This reflects the high binding affinity of SoxR for its target site. Although flash quench can undergo multiple cycles (as long as reduced quencher is present in the solution), SoxR that is bound to DNA can only be oxidized once, after which it can no longer protect the DNA from damage. This oxidized SoxR is unable to equilibrate with reduced SoxR that may be in solution, and damage is able to proceed at guanine sites.

SoxR is unique compared to previously studied proteins in that it is a transcription factor, and oxidation of the protein allows it to activate transcription of its target gene, *soxS* (18). SoxR responds to conditions in the cell that give rise to oxidative radical species in DNA, and here it is demonstrated that one way it can do so is by donating electrons to fill holes that are formed in DNA under these conditions. The subsequent oxidation of SoxR and transcriptional activation of *soxS* form the basis for further study of this protein.

EXPERIMENTAL

DNA synthesis and purification

DNA was synthesized using standard phosphoramidite chemistry on an Applied Biosystems 394 DNA synthesizer. Bases and reagents were ordered from Glen Research. DNA was synthesized trityl on, on a 1 μ mol scale. Following deprotection in NH_4OH , DNA was vacuum dried, dissolved in 15 mM NaPi 50 mM NaCl pH 7.0 buffer, and HPLC purified (Agilent Technologies). The trityl group was manually cleaved with 80% acetic acid, and purified again via HPLC. DNA strands were redissolved in buffer, quantified using UV-Vis (Beckman), and stored at -20°C . The sequences used were PL97A: 5' GAG TAT AAT TGG AGT TCA ATT GAA CTC CTA AAG CGA TTT ATG GAA AAG AGC TCG TAC GAA CGC -3' and its complement, PL158A: 5' TTT TAT AAA CCG CTT TAC CTC AAG TTA ACT TGA GGA ATT A 3' and its complement, and PL213A: the PL158A sequence with a 5' TTT TCC AAT TTT ATA AAT, and its complement.

DNA labeling

DNA was 5' labeled with [^{32}P] γ -ATP and polynucleotide kinase. Labeled DNA was put through Micro Bio spin columns (BioRad), treated with 10% piperidine for 30 min at 90°C , then purified using gel electrophoresis on a 20% polyacrylamide gel (Sequagel). The desired band was visualized using autoradiography, excised, and was eluted into 500 mM NH_4OAc . Labeled DNA was put through spin columns in 5 fractions, spin dried under vacuum, and stored at -20°C until hybridization.

[Ru(phen)(dppz)(bpy')]Cl₂

[Ru(phen)(dppz)(bpy')]Cl₂ was synthesized according to procedures previously outlined. (19, 20). [Co(NH₃)₅Cl]Cl₃ and [Ru(NH₃)₆]³⁺ were purchased (Aldrich, Strem). Briefly, [RuCl₃] is reacted with paraformaldehyde in formic acid at 130°C and chilled to form the biscarbonyl

dichloride polymer. The polymer refluxed in methanol with 1,10 phenanthroline to form $[\text{Ru}(\text{phen})(\text{CO}_2)_2\text{Cl}_2]\text{Cl}_2$, recrystallized, and dried under vacuum. The complex is triflated to form $[\text{Ru}(\text{phen})(\text{CO}_2)_2(\text{OTf})_2](\text{OTf})_2$, which is then reacted with dipyrrophenazine in 2-methoxyethanol, precipitated with ammonium hexafluorophosphate (NH_4PF_6), and reprecipitated from acetonitrile with chloroform. 4-butyric acid methyl ester 4'-methyl bipyridine (bpy^{OMe}) is added in with trimethylamine-N-oxide in 2-methoxyethanol at 130°C , and purified on alumina and anion-exchanged to form the chloride salt. Deprotection of the methyl ester is done with LiOH , the solution is acidified, dried using rotary evaporation, and recrystallized with ether from methanol.

Irradiations

DNA was annealed with labeled strand on a heat block from 90°C to room temperature. Solutions were made of DNA, photooxidant, and quencher in $20\ \mu\text{L}$ volumes. Aerobic irradiations were performed in $1.5\ \text{mL}$ eppendorf tubes, and anaerobic irradiations were performed in VWR NMR tubes welded to Teflon coated screw-top lids (J.Young). Samples were irradiated using a $12\ \text{mW}$ LiConix helium cadmium laser at $442\ \text{nm}$.

Gel Electrophoresis

Following irradiation, DNA was cleaved at damage sites by treatment with 10% piperidine for 30 min at 90°C . Samples were spin dried under vacuum. Total radiation was determined using a Beckman LS5000 TD scintillation counter. Samples were dissolved in a denaturing loading dye (80% formamide, 10 mM NaOH in TBE) and run on a 20% polyacrylamide gel at 90 W, in TBE (90 mM Tris-borate, 1 mM EDTA, pH 8.3) for 1-2 hours. Cleavage was compared to standard Maxam-Gilbert sequencing reactions.

Gel Visualization

Gels were scanned using a Storm 820 Phosphorimager (Molecular Dynamics/GE Healthcare) and visualized using ImageQuant (Molecular Dynamics).

SoxR

SoxR was supplied courtesy of Dr. Eunsuk Kim of the Demple group (Harvard School of Public Health) and was expressed and purified according as outlined (21). Protein was stored at -80°C until use. Stocks (49 μ M) were divided into 40 μ L aliquots and stored in storage buffer (50 mM Sodium Phosphate, 300 mM NaCl, 10% glycerol, 0.1% Triton X-100, pH 8.0). For use, one aliquot of SoxR was thawed at room temperature, then analyzed via UV-vis. The sample was then flushed with argon free-flowing over the solution in the cuvette for 30 min. The cuvette was then sealed and transferred to the glove box (Coy Laboratory Products, 98% N₂, 2% H₂ atmosphere). Protein was reduced using sodium dithionite for 10 min. The redox state of the protein was determined using UV-Vis spectroscopy (Beckman). SoxR reduced in this way was used in the experiments.

REFERENCES

1. Dedon, P.C., *Chem. Res. Toxicol.* 21:206-219 (2008).
2. Burrows, C.J., Muller, J.G., *Chem Rev.* 98:1109-1151 (1998).
3. Cadet, J., et al. *Chimia* 62:742-749 (2008).
4. Stemp, E.D.A., Arkin, M.R., Barton, J.K. *J. Am. Chem. Soc.* 119:2921-2925 (1997).
5. Hall, D.B., Holmlin, E.R., Barton, J.K. *Nature* 382:731-735 (1996).
6. Olson, E.J.C., et al. *J. Am. Chem. Soc.* 119:11458-11467 (1997).
7. Delaney, S. et al. *Inorg. Chem.* 41:1966-1974 (2002).
8. Steenken, S., Jovanovic, S.V. *J Am Chem Soc* 119:617-618 (1997).
9. Saito, I. et al. *J Am Chem Soc* 117:6406-6407 (1995).
10. Nunez, M.E., Hall, D.B., Barton, J.K. *Chem. Biol.* 6:85-97 (1999).
11. Schuster, G.B. *Acc. Chem.Res.* 33:253-260 (2000).
12. Guise S.O. *Acc. Chem. Res.* 33:631-636 (2000).
13. Beckman, K.B., Ames, B.N., *J. Biol. Chem.* 272:19633-19636 (1997).
14. Yavin, E. et al. *Proc. Natl. Acad. Sci. USA* 102:3546-3551 (2005).
15. Augustyn, K.E., Merino, E.J., Barton, J.K., *Proc. Natl. Acad. Sci. USA* 104:18907-18912 (2007).
16. Saito, et al. *J. Am. Chem. Soc.* 117:6406-6407 (1995).
17. Gorodetsky, et al. *Proc. Natl. Acad. Sci. USA* 105:3684-3689 (2008).
18. Amabile-Cuevas, C.F., Demple, B. *Nucleic Acids Res.* 19:4479-4484 (1991).
19. Strouse, G.F., et al. *Inorg Chem.* 31:3004-3006 (1992).
20. Anderson, P.A., et al. *Inorg. Chem.* 34:6145-6157 (1995)
21. Chander, M., Demple, B., *J. Biol. Chem.* 279:41603-41610 (2004).

Chapter 4

Light Induced Transcriptional Activation of the *soxS* Gene in *Escherichia coli*

INTRODUCTION

Charge transport (CT) through DNA has been well studied *in vitro*, in well-defined systems containing DNA and various photooxidants. However, only a few studies have examined DNA-mediated CT in cellular contexts, which is important in understanding how feasible this process is in the cellular milieu of various proteins, biomolecules, and small molecules. As has been the case for other studies of DNA-mediated CT, the use of photoactive metal complexes has several advantages over organic oxidants. The modular nature of these complexes allows them to gain functionality by the use of different ligands. The inherent positive charge allows these complexes to enter cells and accumulate near DNA. Finally, photoactivation makes it possible for oxidation to occur in a controlled manner.

Phenanthrenequinone diimine (phi) containing complexes of rhodium are particularly well suited for this chemistry. Of these, $[\text{Rh}(\text{phi})_2\text{bpy}]^{3+}$ has most commonly been used for studies on DNA-mediated charge transport. The phi ligands of this complex are able to intercalate into the base stack, allowing these complexes to bind strongly to DNA at all sites without sequence specificity. This complex also has interesting photophysical properties (1). Irradiation with high-energy light (<300 nm) causes these complexes to perform strand scission at their binding site. Irradiation at >350 nm causes a ligand-centered (LC) excited state on the phi ligand, which is able to inject a hole into DNA. The oxidation potential of this excited state of the related complex $[\text{Rh}(\text{phi})_2\text{phen}]^{3+}$ is >1.8 eV, enough to oxidize guanine residues on DNA. These complexes can oxidize DNA in the absence of an external quencher, reducing the number of components that need to be present inside the cell for photooxidation to occur. The trade-off is the decreased quantum yield of damage, as the excited state has a short lifetime compared to the long lived ground state Ru photooxidants (2).

In studies on intact isolated nuclei and mitochondria, $[\text{Rh}(\text{phi})_2\text{bpy}]^{3+}$ has been shown to effectively enter these organelles and cause oxidative damage to the DNA. In these studies, $[\text{Rh}(\text{phi})_2\text{bpy}]^{3+}$ is irradiated at a mixture of wavelengths, such that the complex both cleaves at its

binding site and performs long range hole transfer to form oxidative lesions. Importantly, oxidative damage is turned into strand breaks only in the presence of enzymes that are able to cut the sugar-phosphate backbone, or by treatment with base, such as piperidine. By examining the different damage patterns for piperidine treated and untreated DNA, the location of oxidative lesions distal to the Rh binding sites can be determined. Consistent with earlier studies, these lesions occur at guanine rich “hot spots,” areas of low oxidation potential. Furthermore, damage is localized at the 5' end of guanine doublets and triplets, which is a characteristic signature of DNA damage due to hole transport through the base stack. These results indicate that $[\text{Rh}(\text{phi})_2\text{bpy}]^{3+}$ is able to cross lipid membranes and enter organelles, and effect similar oxidative chemistry on DNA as has been shown for *in vitro* studies (3, 4).

The purpose of this study is to determine whether oxidative radicals in DNA are able to serve as a signal for activating the transcription of *soxS* by SoxR in bacterial cells. Previously it has been shown that reduced SoxR is able to donate an electron to fill a hole photochemically generated in DNA, attenuating damage at guanine residues, whereas oxidized SoxR cannot. Given these results, it is likely that the reduced SoxR can be oxidized by guanine radicals converting to its transcriptionally active form. Thus, when bacterial cells are placed under the same conditions that generate migratory oxidative radicals in DNA, i.e., irradiation in the presence of the photooxidant $[\text{Rh}(\text{phi})_2\text{bpy}]^{3+}$, some of the holes should be able to migrate to SoxR and oxidize it, causing it to activate transcription of its target gene (Figure 4.1).

To improve the sensitivity of these experiments, reverse-transcriptase polymerase chain reaction (RT-PCR) was employed to amplify the *soxS* transcript (Figure 4.2). Cultures grown under different conditions were pelleted, lysed, and total RNA was extracted. The

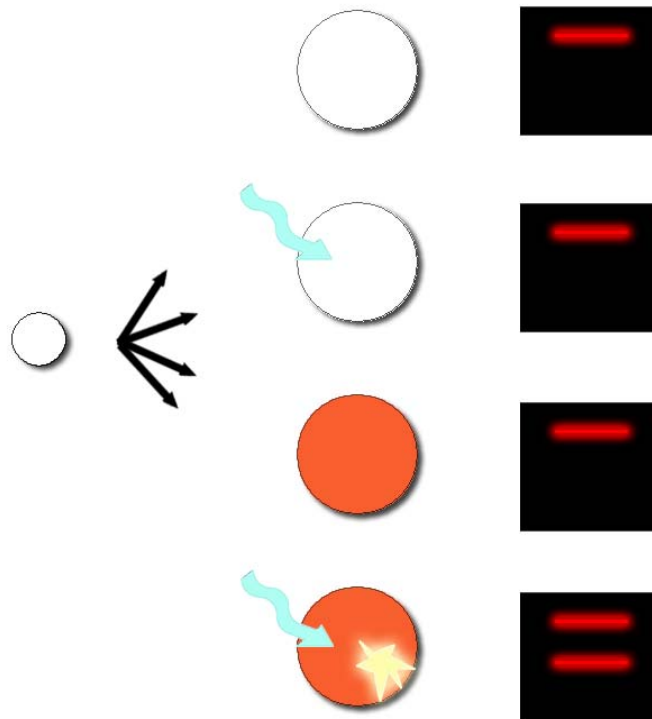


Figure 4.1: Schematic for assaying cells for *soxS* transcript in response to DNA oxidation. Cultures are grown from a single colony in media (white) or media containing [Rh(phi)₂bpy]³⁺ (orange), and cultures are either irradiated (blue arrows) or kept in the dark. Only cultures irradiated in the presence of photooxidant will undergo DNA damage. If SoxR is oxidized and able to activate transcription in response to oxidative radicals in DNA, the sample treated with both photooxidant and light should show a RT-PCR band corresponding to the *soxS* transcript in addition to the internal 23S control transcript.

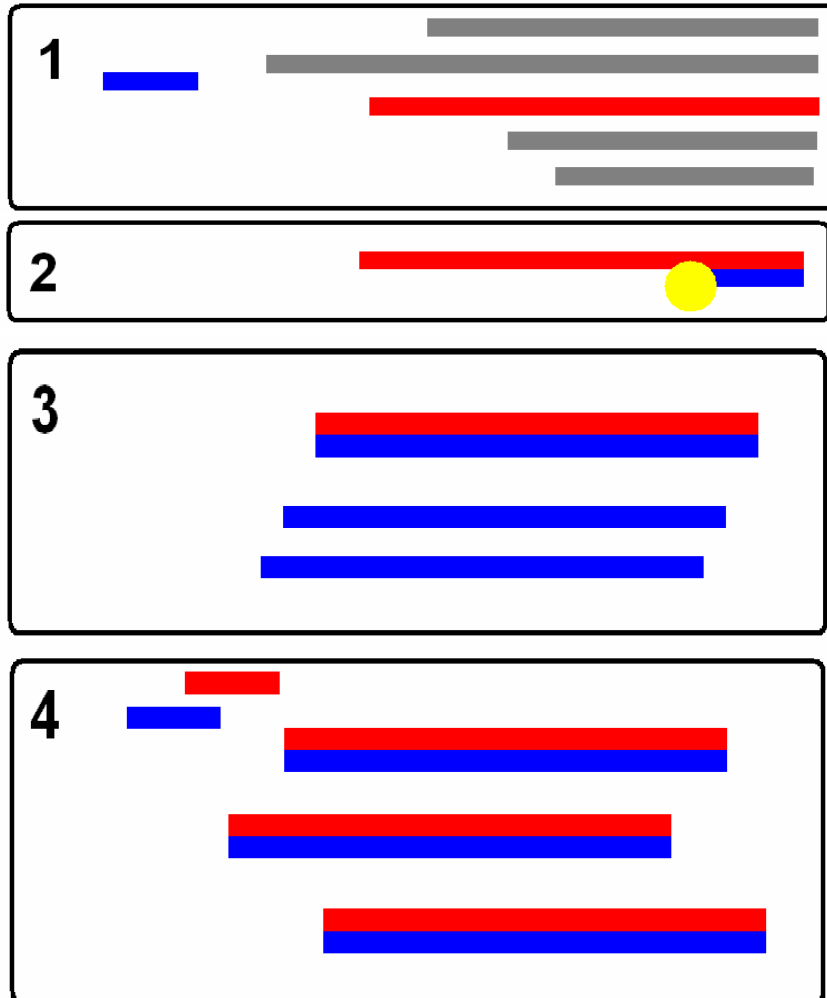


Figure 4.2: The procedure for reverse transcriptase polymerase chain reaction (RT-PCR) is illustrated here. A total RNA extract (grey) is incubated with a DNA primer (blue) complementary for an mRNA transcript of interest (red). Reverse transcriptase (yellow) makes a DNA copy only of the mRNA transcript hybridized to the primer, creating a cDNA library. The resulting cDNA is amplified using PCR to form a double stranded DNA copy of the original gene.

RNA is then incubated with a DNA primer complementary to the 3' end of the transcript of interest; in this case, it is the *soxS* transcript. Reverse transcriptase is then used to create a cDNA copy of the mRNA transcript. PCR is employed using primers complementary to the ends of this cDNA, amplifying the transcript as double-stranded DNA, which is analyzed using agarose gel electrophoresis. As an internal control, the 23s subunit of the *E. coli* ribosome was amplified in the same mixtures; the levels of this RNA are not expected to change due to the conditions tested, and the amount of *soxS* transcript can be reported as relative to this internal control.

RESULTS

In order to produce a high yield of oxidative damage, a high intracellular concentration of $[\text{Rh}(\text{phi})_2\text{bpy}]^{3+}$ is desired; however, there is a threshold beyond which cell growth is inhibited. To investigate the dependence of cell growth and transcription on $[\text{Rh}(\text{phi})_2\text{bpy}]^{3+}$, a starter culture of *E. coli* was grown from a single colony overnight and used to inoculate 1 mL of LB containing $[\text{Rh}(\text{phi})_2\text{bpy}]\text{Cl}_3$ at different concentrations. The cultures were allowed to grow for 8 hours, after which optical densities were taken. The cells were pelleted and resuspended in NCE, irradiated for 60 min, and total RNA was extracted and purified. Uptake of the $[\text{Rh}(\text{phi})_2\text{bpy}]^{3+}$ is evidenced by a deep brownish-red color of the cell pellet. Irradiations were done with a 340 nm filter to prevent direct strand cleavage by the photooxidant, which occurs upon irradiation with light of 313 nm. RT-PCR was performed on the samples, and the resulting DNA was run out on agarose.

Figure 4.3 shows the effect of rhodium concentration on cell growth and the relative amount of *soxS* transcript versus the 23s band. Optical density remains fairly constant across the concentration range, up to 100 μM , and cells grown in 500 μM show a sharp decrease in growth. A comparison of the relative *soxS* transcript levels shows an increase in *soxS* expression, up until 500 μM $[\text{Rh}(\text{phi})_2\text{bpy}]^{3+}$, where the transcript level is dramatically

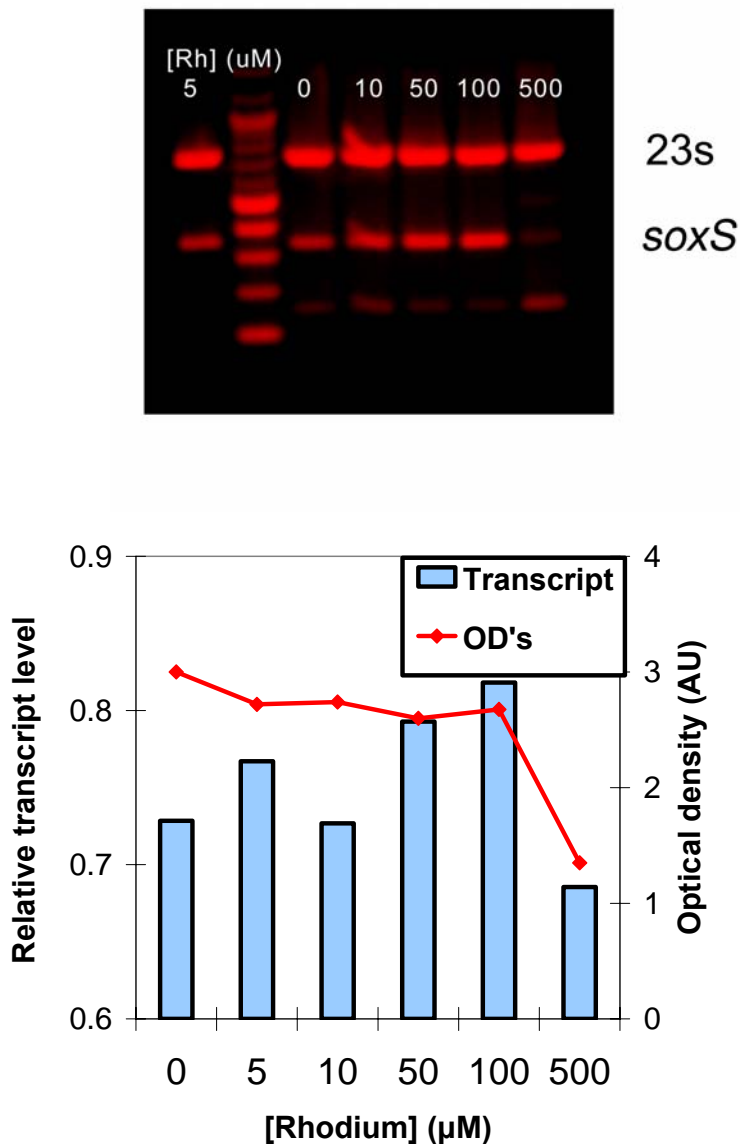


Figure 4.3: A comparison of *soxS* expression and optical densities in *E. coli* at different concentrations of $[\text{Rh}(\text{phi})_2\text{bpy}]^{3+}$. Top: An agarose gel image of RT-PCR products stained with ethidium bromide is shown. The top band is a 23s internal control. The bottom band is the *soxS* transcript. The lowest molecular weight band is free primer. Cells were grown in the indicated concentrations of $[\text{Rh}(\text{phi})_2\text{bpy}]\text{Cl}_3$ for 8 hours before being measured for optical density (OD) and assaying for *soxS* transcription. Bottom: A comparison of OD (red lines) and relative transcript level (blue bars) shows that both decrease sharply at concentrations of $[\text{Rh}(\text{phi})_2\text{bpy}]^{3+}$ above 100 μM. Cells numbers were normalized prior to assaying for transcript.

decreased. It is interesting to note that transcript levels increase while ODs remain consistent, indicating *soxS* transcript levels are a function of the concentration of photooxidant and is independent of cell growth. Furthermore, these results suggest that $[\text{Rh}(\text{phi})_2\text{bpy}]^{3+}$ at high concentrations has a negative effect on cell growth that is independent of its role as a photooxidant, as cultures showed a decrease in growth even prior to irradiation.

Transcript levels of *soxS* were also investigated for samples irradiated for various lengths of time. Cells were grown as described previously, and were irradiated for 10, 30, and 60 min. Longer irradiations should increase the number of oxidative events, thus increasing the number of SoxR proteins oxidized and the transcript levels of *soxS*. RNA extraction and RT-PCR were performed in the same manner as described previously, again using the 23s rRNA as an internal control. Figure 4.4 shows the results of this experiment. First, the gel shows equal amounts of 23s DNA for each sample, indicating that the bacteria were expressing the comparable total RNA. The untreated sample, the sample containing $[\text{Rh}(\text{phi})_2\text{bpy}]^{3+}$ and not irradiated (DC), and the sample lacking the photooxidant but irradiated (LC) do not show significant *soxS* expression. However, samples containing $[\text{Rh}(\text{phi})_2\text{bpy}]^{3+}$ show evidence of strong *soxS* expression upon irradiation, which increases with the duration of irradiation. Under these irradiation conditions, and estimating an intracellular $[\text{Rh}(\text{phi})_2\text{bpy}]^{3+}$ concentration of 5 μM , 1 oxidation event to generate guanine radicals is expected to occur every 300 bp; note that only some of the guanine radicals will lead to irreversible guanine lesions, such as 8-oxo-guanine. Nonetheless, since the Rh photooxidant preferentially causes DNA damage (2), these results indicate that SoxR can be activated in cells by DNA oxidation. Rather than reactive oxygen intermediates inducing SoxR directly, it appears that guanine radicals in DNA can trigger its activation.

To ensure that the expression of *soxS* under these conditions is consistent with previous studies of SoxR, the levels of SoxR activation by Rh photoactivation was compared with that by an equal concentration of methyl viologen, a commonly used activator of SoxR (Fig 4.5) (5).

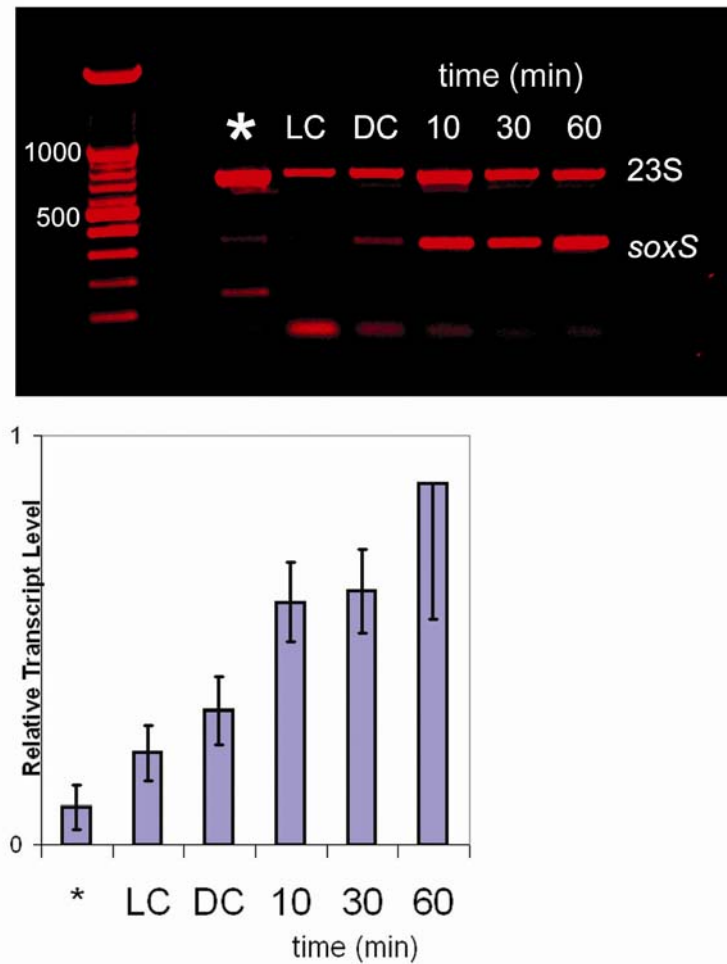


Figure 4.4: The transcript levels of *soxS* are significantly higher for samples that are irradiated in the presence of $[\text{Rh}(\text{phi})_2\text{bpy}]^{3+}$ than in either the control lacking the photooxidant or the control that is not irradiated. Transcript levels also seem to increase with increasing irradiation times; however at long irradiation times transcript levels have high deviations. Top: An agarose gel of RT-PCR products stained with ethidium bromide is shown. The higher and lower molecular weight bands correspond to the 23s and *soxS* RNAs, respectively. Bottom: Levels of *soxS* bands quantified as the ratio of *soxS* transcript to the 23s internal control. Error bars represent the standard error of the average of 3 separate trials.

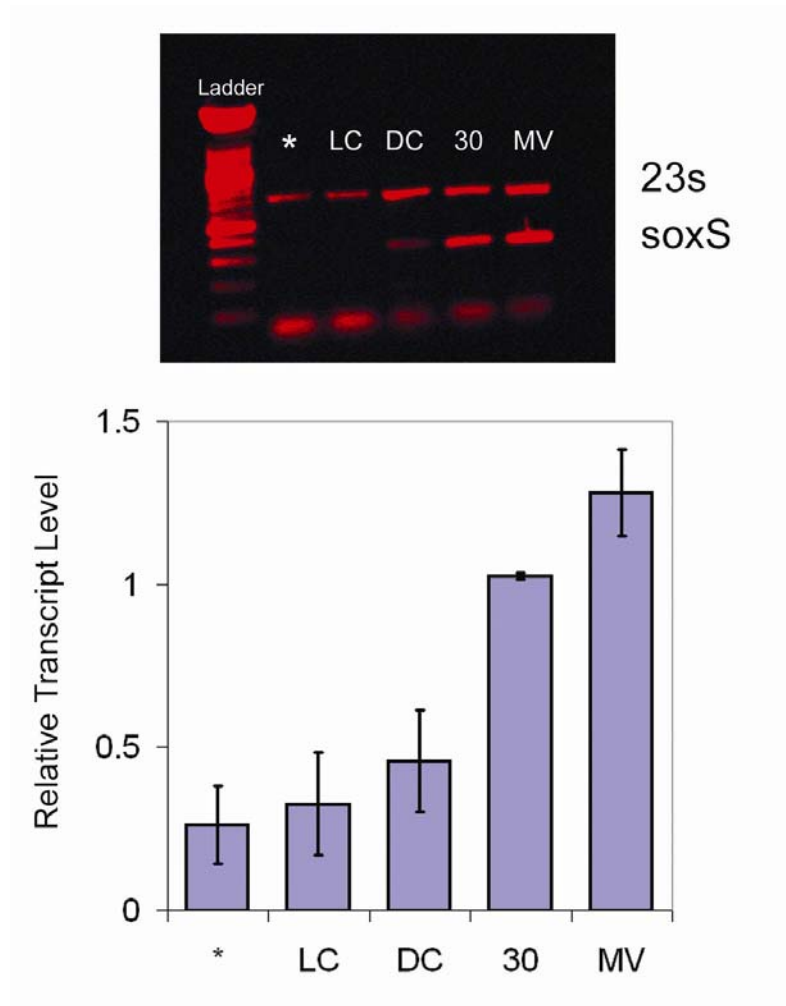


Figure 4.5: The transcript levels of *soxS* are comparable for samples that are irradiated for 30 min in the presence of $[\text{Rh}(\text{phi})_2\text{bpy}]^{3+}$ and those that are shaken aerobically with the same molar concentration of methyl viologen for 30 min. Top: An agarose gel of RT-PCR products stained with ethidium bromide is shown. The higher and lower molecular weight bands correspond to the 23s and *soxS* RNAs, respectively. Bottom: Levels of *soxS* bands quantified as the ratio of *soxS* transcript to the 23s internal control. Error bars represent the standard error of the average of 4 separate trials.

It should be noted that the methyl viologen-treated samples were tested aerobically with active shaking of the cultures, while Rh-treated samples were irradiated in 24-well plates without aeration. Despite these different conditions, the expression levels of *soxS* in the samples treated with Rh are quite close to those found upon incubation of this *E. coli* strain with methyl viologen. Unlike the strains used in some previous studies, SoxR is not overexpressed in this wild-type strain.

DISCUSSION

Several transition metal octahedral complexes have been shown to be able to enter cells (6), and much ongoing research is aimed toward developing complexes that are able to bind and cleave DNA specifically at mismatch sites in cells (7). However, $[\text{Rh}(\text{phi})_2\text{bpy}]^{3+}$ binds DNA with low sequence specificity and furthermore is able to oxidize DNA when it is intercalated into the DNA base stack. Like dppz complexes of Ru, this damage occurs as a consequence of formation of base radicals that are able to migrate through the DNA base stack and localize at guanine sites, giving it a long-range characteristic. Unlike the Ru complexes, $[\text{Rh}(\text{phi})_2\text{bpy}]^{3+}$ is a strong excited state photooxidant, which means that it does not require an external quencher in order to oxidize DNA, and will not generate diffusible radical species. These cell entry and photooxidant properties of $[\text{Rh}(\text{phi})_2\text{bpy}]^{3+}$ make it an ideal candidate for the study of long-range oxidative damage in vivo.

Here, $[\text{Rh}(\text{phi})_2\text{bpy}]^{3+}$ and light are used to controllably generate migratory radicals in DNA akin to what may happen to the cell in the presence of increased levels of reactive oxygen species. The activation of genes thought to respond to these conditions is then assayed. In this example, the transcription factor SoxR contains two $[\text{2Fe2S}]^{1+/2+}$ clusters, which, when oxidized, cause the protein to act as a transcriptional activator. The relevant 1+/2+ redox couple of the $[\text{2Fe2S}]$ clusters of DNA-bound SoxR occurs at +200 mV vs NHE (8). This potential allows SoxR to remain in its reduced form in the cell but still be able to respond to conditions of

oxidative stress. Importantly, guanine radicals in DNA have redox potentials high enough to readily oxidize the clusters of SoxR.

It appears as though bacteria are able to take up $[\text{Rh}(\text{phi})_2\text{bpy}]^{3+}$ when it is present in their growth medium, although the actual intracellular concentration was not determined. Growth levels remained constant at lower concentrations of complex, but showed a marked decrease at higher concentrations ($>100 \mu\text{M}$). Levels of *soxS* increased with $[\text{Rh}(\text{phi})_2\text{bpy}]^{3+}$ concentration but also decreased at higher Rh concentrations. These differences in the RT-PCR assay are independent of cell growth as ODs were normalized just prior to irradiation. Interestingly, the 23s rRNA band remains constant even at $500 \mu\text{M}$ $[\text{Rh}(\text{phi})_2\text{bpy}]^{3+}$, whereas the *soxS* band decreases. This suggests that while high concentrations of $[\text{Rh}(\text{phi})_2\text{bpy}]^{3+}$ may slow down cell proliferation, the cells themselves are functional, with high ribosomal RNA levels. Once treated with both $[\text{Rh}(\text{phi})_2\text{bpy}]^{3+}$ and light, however, the high presence of oxidizing species may cause cell death and a decrease in transcript levels. Finally, the residual *soxS* transcript level seen in the absence of $[\text{Rh}(\text{phi})_2\text{bpy}]^{3+}$ may be due to amplification of the genomic *soxS* gene; in subsequent experiments, this was eliminated by the addition of a DNase digestion step during RNA purification.

In addition to *soxS* transcript levels increasing as a function of $[\text{Rh}(\text{phi})_2\text{bpy}]^{3+}$ concentration, they also are demonstrated to increase as a function of irradiation time. Untreated cell samples, samples treated with $[\text{Rh}(\text{phi})_2\text{bpy}]^{3+}$ but not irradiated (DC), and samples irradiated in the absence of $[\text{Rh}(\text{phi})_2\text{bpy}]^{3+}$ (LC), do not exhibit *soxS* transcription, whereas cells treated with both $[\text{Rh}(\text{phi})_2\text{bpy}]^{3+}$ and light transcribe *soxS*. This effect increases with irradiation time, as expected; samples irradiated for 30 min show higher transcript levels than those irradiated for 10 min, and this trend continues for the 60 min samples, although the deviation at this long irradiation length is high. In general, higher $[\text{Rh}(\text{phi})_2\text{bpy}]^{3+}$ concentrations permit a higher quantum yield of damage, and longer irradiation times lead to more opportunities for damage to

occur; thus these results indicate *soxS* transcription is related to the formation of oxidative radicals in DNA. Under these conditions, we estimate a 10% efficiency of cellular entry, and a 10% quantum yield based on actinometry measurements. Interestingly, it is estimated that a hole will be generated in the DNA every 300 base pairs, which within the theoretical distance over which DNA-mediated charge transport must occur to be biologically useful.

Importantly, the only known activator of *soxS* transcription is SoxR, making it highly probable that oxidation of SoxR by guanine radicals is the mechanism by which *soxS* transcript levels are increased. To further confirm this, the transcriptional activation due to Rh and light was compared to that due to methyl viologen, a well studied activator of SoxR (5). Indeed, *soxS* transcript levels are comparable whether cells are treated with Rh and light for 30 min, or whether they are shaken aerobically with an equal concentration of methyl viologen. Thus both methyl viologen and $[\text{Rh}(\text{phi})_2\text{bpy}]^{3+}$, which can activate SoxR only through intermediate DNA oxidation, promote *soxS* expression to a similar extent.

Thus it is clear that SoxR can be activated through DNA damage without the intermediary of diffusible radicals. Instead, guanine radicals may serve as the one-electron oxidant for SoxR within the cell.

EXPERIMENTAL*[Rh(phi)₂bpy]Cl₃*

[Rh(phi)₂bpy]Cl₃ was prepared according to (9, 10, 11). Briefly, RhCl₃ was refluxed with KCl in methanol, and bpy (2,2' dipyridyl) was added to form [Rh(bpy)Cl₄]Cl₃. The product was filtered as a yellow solid, washed with acetone, and dried. The product was then dissolved in concentrated triflic acid, and precipitated with ether to form [Rh(bpy)(OTf)₄](OTf)₃ as a brown oil. This was refluxed in ammonium hydroxide, and dried to form [Rh(bpy)(NH₃)₄](OTf)₃. This yellow solid was dissolved in 50:50 water:acetonitrile, phenanthrenequinone was added, and the solution was made basic with the addition of excess NaOH to form a deep reddish brown solution of [Rh(phi)₂bpy](PF₆)₃. The reaction was worked up with HCl, dried under rotary evaporation, and precipitated with ammonium hexafluorophosphate (NH₄PF₆). Excess ligand was removed using a SepPak, and the complex was column purified using silica and dichloromethane with 10% methanol, and anion exchanged with KCl to form the final product.

RT-PCR primers

The primers used for reverse transcription were 5' CCGCTTTATCGTTACTTATG 3' for the 23s ribosomal RNA, and 5' ATTACAGGCGGTGGCGATAA 3' for the *soxS* transcript. The same primers were used for PCR, with the addition of 5' CAGCGACTTATATTCT GTAG 3' for the 23s RNA and 5' ATGTCCCATCAGAAAATTAT 3' for the *soxS* transcript.

Effect of [Rh(phi)₂bpy]³⁺ on cell growth

E. coli strain K-12 TB1 (New England Biolabs) was streaked to a Luria-Bertani (LB) agarose plate, and a starter culture was grown from a single colony. A 50 μL aliquot of this starter culture was used to inoculate 1 mL LB or LB containing the indicated concentrations of [Rh(phi)₂bpy]Cl₃.

Cells were grown for 8 hours, at which time an optical density was taken as the absorbance at 600 nm. The cells were pelleted via centrifugation, and resuspended in NCE. Irradiations were carried out using a solar simulator (Oriel Instruments) using a 340 nm internal low pass filter and a 320 nm external low-pass filter. Total RNA was extracted using a RNeasy kit (Qiagen). Reverse transcription PCR was carried out using the OmniScript system (Qiagen) using the 23s and *soxS* primers and the resulting cDNA was PCR-amplified using standard procedures (Roche).

Effect of [Rh(phi)₂bpy]³⁺ and light on soxS transcript levels

E. coli strain K-12 TB1 (New England Biolabs) was streaked to a Luria-Bertani (LB) agarose plate, and a starter culture was grown from a single colony. A 50 µL aliquot of this starter culture was used to inoculate 5 mL LB or LB containing the indicated concentrations of [Rh(phi)₂bpy]Cl₃. Cells were grown for 4-5 hours, at which time an optical density was taken as the absorbance at 600 nm. The cells were pelleted via centrifugation, and resuspended in NCE to equal dilutions based on their ODs. Irradiations were carried out using a solar simulator (Oriel Instruments) using a 340 nm internal low-pass filter and a 320 nm external low-pass filter. Immediately after irradiation, cells were frozen in liquid N₂. Samples were thawed at 60° C, and RNA was extracted using a RNeasy kit (Qiagen), during which an on column DNase digestion was performed (Qiagen). Reverse transcription PCR was carried out using the OmniScript system (Qiagen) using the 23s and *soxS* primers and the resulting cDNA was PCR-amplified using standard procedures (Roche).

Methyl viologen treatment of samples

E. coli strain K-12 TB1 (New England Biolabs) was streaked to a Luria-Bertani (LB) agarose plate, and a starter culture was grown from a single colony. A 50 µL aliquot of this starter culture was used to inoculate 1 mL LB containing 50 µM methyl viologen (Aldrich). The sample was

shaken aerobically at 220 rpm for 30 min, after which it was immediately frozen in liquid N₂.

Samples were then thawed and assayed as described previously.

REFERENCES

1. Turro, C. et al, *Inorg. Chim. Acta.* 243:101-108 (1996).
2. Hall, D.B., Holmlin, L.F., Barton, J.K. *Nature* 382:731-735 (1996).
3. Nunez, M.E., Holmquist, G.P., Barton, J.K. *Biochemistry* 40:12465-12471 (2001).
4. Merino, E.J., Barton, J.K. *Biochemistry* 47:1511-1517 (2008).
5. Amabile-Cuevas, C.F., Demple, B. *Nucleic Acids Res.* 19:4479-4484 (1991).
6. Puckett, C.A., Barton, J.K., *J. Am. Chem. Soc.* 129:46-47 (2007).
7. Ernst, R.J., Song, H., Barton, J.K. *J. Am Chem. Soc.* 131:2359-2366 (2009).
8. Gorodetsky, A.A. et al. *Proc. Natl. Acad. Sci. USA* 105:3684-3689 (2008).
9. Sitlani, A., Barton, J.K. *Biochemistry* 33:12100-12108 (1994).
10. Pyle, A.M., Chiang, M.Y., Barton, J.K. *Inorg. Chem.* 29:4487-4495 (1990).
11. Lee, J.R. et al. *J. Chin. Chem. Soc.* 50:227-232 (2003).

Chapter 5

In Vitro Transcriptional Activation of *soxS* from a
Distance by DNA-Mediated SoxR Oxidation

INTRODUCTION

It has thus far been demonstrated that the oxidation state of the [2Fe2S] clusters in SoxR is sensitive to charges migrating through the base stack of DNA. Electrochemistry can be performed on the DNA bound protein, using the DNA itself as the means to transfer charge between the cluster and electrodes. The major persistent oxidative species in DNA, migratory radicals, are also able to travel through this electronic assembly and access the [2Fe2S] clusters as well. In cells, the formation of these radicals in the DNA causes activation of the target gene of SoxR, *soxS*, most likely by DNA-mediated oxidation of SoxR.

However, these studies do not directly demonstrate the oxidation of SoxR from a distance. UV-vis spectroscopy can be used to monitor the increase in absorbance of the oxidized form of SoxR between 320 and 540 nm; however, these extinction coefficients are small, making it difficult to monitor small changes in the amount of oxidized SoxR (1). Another method is to monitor the EPR signal of SoxR; the reduced form of the protein has a signal with g-values of 2.01, 1.92, and 1.90, whereas the oxidized form of SoxR is EPR-silent (1). This technique has successfully been used to study the oxidation state of SoxR in cells overexpressing this protein (2). The disadvantages of this method are the large amounts of protein required to observe a large EPR signal, and that the disappearance of the EPR signal may be due to the protein being oxidized, or other factors such as sample degradation. On the other hand, assaying for the transcriptional activity of SoxR is an attractive way of observing its oxidation, because it is a “turn-on” signal, it is biologically relevant, and it ensures that the resulting oxidized protein is indeed active. Furthermore, these assays are very sensitive as they involve detection of a radiolabeled transcript; thus, only small amounts of SoxR are required to observe a quantifiable signal.

In vitro transcription assays

In vitro transcription assays are used to investigate conditions under which a transcription factor is able to turn on its target gene(s). They typically involve several components: (i) DNA that contains both the gene of interest and the binding region for the transcription factor is synthesized or PCR amplified; (ii) the transcription factor itself in a pure form; (iii) the signaling molecule(s) or process(es); (iv) RNA polymerase; and (v) an assay buffer that contains the ribonucleotides (NTPs), Mg^{2+} , and in some cases a starting dinucleotide. The components are combined, and transcription is allowed to proceed at 37°C. After an allotted time, a stop buffer containing EDTA is added to chelate the Mg^{2+} and halt transcription.

Transcription can either create a full length transcript, which involves the presence of all four nucleotides, or, in an abortive assay in which one or more of the four nucleotides is missing from the reaction mixture, a truncated transcript. In an abortive transcription assay, the RNA polymerase remains trapped at the transcription start site, and the rate of product formation is directly dependent on the number of promoters that are occupied by polymerase in an open complex. Full length transcription is used to locate transcription starts and qualitatively the activity of transcription factors, whereas abortive transcription assays provide information on the rate of transcript formation, thus providing a quantitative measure of transcription (3).

The mRNA transcript formed in these assays is detected in various ways, almost always involving the incorporation of radiolabeled nucleotides. In full length assays, this can be in a “hot” or “cold” labeling method. Hot labeling involves the incorporation of a radiolabeled nucleotide in the initial transcription assay mixture; the resulting message is analyzed using denaturing PAGE followed by autoradiography. Cold labeling involves using RT-PCR to amplify the transcript and analyzing the resulting DNA copy of the gene on a non-denaturing agarose gel. Abortive transcription assays use the hot labeling method to incorporate a radiolabeled nucleotide into the truncated message, which is then detected using denaturing PAGE followed by autoradiography (4). Recently, methods have been developed to quantify

transcript levels by incorporation of fluorescent nucleotides; however, it is possible that the rate and yield of incorporation of these nucleotide analogues will be different than that of native nucleotides.

Troubleshooting transcription assays

The multiple components necessary for *in vitro* transcription makes it difficult to troubleshoot. It is important that each component be made in RNase free buffer; RNase is a hardy enzyme that is commonly deactivated using diethylpyrocarbonate (DEPC) followed by autoclaving. However, care must be used when using DEPC-treated water for *in vitro* transcription assays as buffers made with DEPC-treated water have been shown in some cases to inhibit transcription. Using commercially available RNase-free water or reverse-osmosis purification under strict RNase-free conditions will circumvent the issues raised by DEPC treatment. Similarly, all equipment, such as pipettes, pipette tips, vials, and glassware, must be cleaned or purchased as RNase free; protocols for removing RNase from pipettes and glassware have been documented in literature.

E. coli RNA polymerase is a holoenzyme complex which consists of four subunits, 2α , β_1 , and β_2 , and a sigma factor, which imparts specificity at certain types of promoters (5). RNA polymerase is commercially available as both the sigma-free and sigma-saturated enzyme. It is important to note that high concentrations of RNA polymerase will decrease specificity in transcription assays, especially in the case of transcriptional repressors, where it will outcompete binding of the repressor for DNA. Polymerase must therefore be diluted from the stock solution before use. On the other hand, the activity of RNA polymerase decreases as its concentration approaches the dissociation constant of the subunits of the holoenzyme. RNA polymerase should be diluted to no less than a concentration of 0.01 $\mu\text{g/mL}$, and stored at -80°C until use. Finally, The Mg^{2+} cation is necessary for RNA polymerase activity; transcription stop buffers contain

high concentrations of EDTA, which chelates Mg^{2+} . However, at high concentrations of Mg^{2+} , RNA polymerase loses its specificity, and increased background transcription may be observed.

When working with template DNA containing more than one promoter region, starting dinucleotides confer additional specificity, as they bind to the correct +1 start site and allow RNA polymerase to initialize transcription. Ideally, the concentration of the dinucleotide should be 10 to 20× the concentration of the other nucleotides, to prevent initiation by the other nucleotides present in solution. Insufficient or impure dinucleotide can cause multiple bands (background bands) to be seen even in the presence of active transcription factor. Dinucleotide can be purchased or custom-made, transferred to single-use aliquots, dried by vacuum centrifugation, and stored at $-20^{\circ}C$. For the studies described here, the best results have been seen with custom made dinucleotides which were deprotected less than 24 hrs prior to the assay, and dissolved in the transcription buffer immediately prior to use.

Transcription studies on SoxR

Both full length and abortive transcription assays have been used to identify the conditions necessary for transcription by SoxR. An abortive transcription assay on linear DNA was used to determine that the cluster of SoxR is necessary for transcription; this was confirmed using full length transcription followed by primer extension on a supercoiled plasmid (6, 7). Full-length transcription from either linear or supercoiled plasmid as the template DNA was used to demonstrate the redox-dependent activity of SoxR. These prior studies demonstrate that a variety of *in vitro* transcription assays are viable for the study of SoxR, and are sensitive enough to observe its redox activity (8, 9).

Building on this body of work, the current study aims to observe the one-electron oxidation of SoxR by guanine radicals formed by the photoexcitation of $[Rh(\text{phi})_2\text{bpy}]^{3+}$, covalently attached to one end of the DNA duplex containing the SoxR binding site and *soxS* gene (Figure 5.1). Oxidized SoxR in turn is a strong transcriptional activator of the *soxS* gene as

it is able to recruit RNA polymerase to the promoter region of *soxS*. Previous studies have demonstrated the electronic accessibility of the [2Fe2S] clusters to the DNA base stack; reduced SoxR is able to donate an electron to fill holes in DNA that otherwise become trapped to form oxidative lesions on guanine residues, and one-electron photooxidation of DNA in cells can cause them to induce the transcription of *soxS*. This mechanism by which SoxR can be activated can explain how it is able to sense conditions of oxidative stress in cells while remaining bound to DNA, by using the DNA itself as an antenna to gain information about oxidative events occurring in the larger space of the cytoplasm.

An *in vitro* assay allows the oxidation of SoxR to be directly attributed to the formation of holes in DNA from a distance; the covalent tethering of the [Rh(phi)₂bpy]³⁺ to a position 80 base pairs away from the site of SoxR binding makes the DNA a necessary medium through which this oxidative signal must travel. Importantly, photoexcitation of this metallocomplex does not generate any reactive oxygen species, which might oxidize SoxR in a diffusion dependent manner.

In order to study the efficiency of oxidation of SoxR by DNA-mediated charge transfer, it is important to be able to quantify the *soxS* transcript that is formed, and therefore an abortive transcription assay was chosen for these studies. This truncated transcript is radiolabeled by the incorporation of $\alpha^{32}\text{P}$ -labeled uridine triphosphate (UTP), separated from free UTP and background transcript bands by denaturing PAGE, and quantified by autoradiography of the gel. These studies reveal that *soxS* transcript is indeed seen when reduced SoxR is oxidized from a distance by the long-range migration of holes from the initial site of oxidation through the DNA to the redox-sensitive metal clusters of the protein.

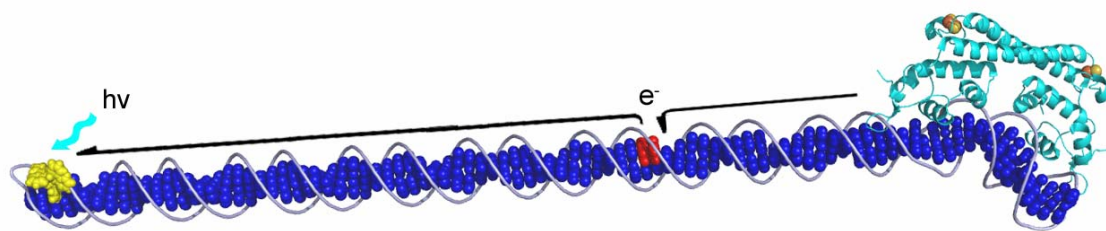


Figure 5.1: Schematized model of transcriptional activation of SoxR from a distance through DNA-mediated charge transport. Here a tethered metal complex (yellow) is used to inject an electron hole into the DNA base pair stack (dark blue) so as to generate a guanine radical (red). DNA-mediated charge transport from SoxR (light blue), bound at its promoter site, to the guanine radical fills the hole and leads to oxidation and activation of SoxR. The SoxR structure shown is based on the crystal structure of oxidized SoxR bound to DNA (10).

RESULTS

Guanine oxidation in the 180-mer PCR template DNA

The transcription template DNA is a 180-mer linear duplex containing the SoxR binding site, the +1 transcription start site for *soxS*, and a portion of the *soxS* gene. This DNA is PCR amplified from *E. coli* genomic DNA using two primers, one of which is covalently modified at the 5'-end with the photooxidant $[\text{Rh}(\text{phi})_2\text{bpy}]^{3+}$ (see experimental). The sequence and resulting duplex are shown in Figure 5.2 and 5.3. Photoexcitation of $[\text{Rh}(\text{phi})_2\text{bpy}]^{3+}$ and the creation and transport of holes through the duplex was examined via the formation of guanine radicals and their subsequent trapping to form permanent guanine oxidation products. For this experiment, the opposite primer is $\gamma^{32}\text{P}$ - radiolabeled at the 5'-position, resulting in the full length radiolabeled PCR product. After irradiation, the DNA is treated with piperidine, which produces strand breaks at sites of base oxidation. The resulting DNA fragments are separated using denaturing sequencing PAGE, imaged using autoradiography, and the location of the DNA base damage is visualized as bands. Figure 5.4 shows the results of this analysis. Guanine oxidation, in general, is hard to visualize, but at 30 and 60 min of irradiation, damage products are seen, especially at a 4-guanine site halfway down the duplex. One reason for the low yield of damage is that the holes need to equilibrate over all the guanine sites in the duplex; thus the average yield of damage at each guanine is low. Importantly, there is an even distribution of damage observed in this experiment. Damage is not preferential to the end of the DNA containing the tethered photooxidant. It appears that charge can efficiently travel through the entire length of this 180-base pair DNA duplex, equilibrating at sites of low oxidation potential, notably a "hot spot" of 4 consecutive guanine residues ~20 base pairs away from the site of SoxR binding.

5' **ctgaataattttctgatggg**acataaatctgcctcttttcagtgttcagttcgttaat
 tc*atcT*gttggggagtataatt**cctcaagttaacttgagg**taaagcgatttatggaaaag
 aaattaccccgcattaaagcgctgctaaccccggcgaagtg**gcgaaacgcagcgggtg**
gc 3'

Figure 5.2: The sequence of the 180 base pair transcription template is shown. The primer regions are shown in red. The 3' primer is modified with $[\text{Rh}(\text{phi})_2\text{bpy}]^{3+}$. The SoxR binding site is in bold. The +1 transcription site and transcribed region is shown in blue italics.



Figure 5.3: Schematized model for the long range photooxidation of the transcription template. [Rh(phi)₂bpy']³⁺ covalently tethered to one end of the duplex is irradiated with light to form an excited state photooxidant, generating holes in the DNA. The SoxR binding footprint is shown in blue, and the protein binds 80 bp away from site of Rh intercalation, which is 2 bp into the duplex.

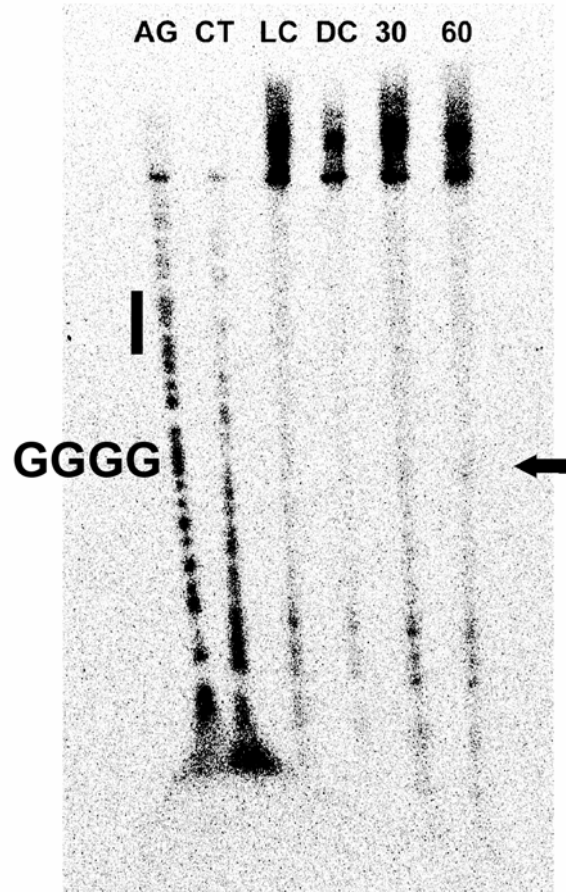


Figure 5.4: Guanine oxidation is shown in a 10% polyacrylamide gel. AG and CT are Maxam-Gilbert sequencing lanes. Light control (LC) is the 180-mer transcription template PCR amplified using unmodified primer B (see experimental). Dark control (DC) is the Rh-modified transcription template, not irradiated. Numbers indicate time (min) of irradiation. The arrow indicates the location of a GGGG site in the duplex. The SoxR binding site is indicated by the black bar. Lower molecular weight bands may reflect polymerase stop positions.

Transcriptional activation by SoxR

Oxidized SoxR is a strong activator of the *soxS* gene. To examine this transcriptional activity in the *in vitro* abortive transcription assay, oxidized SoxR was incubated with the unmodified 180-mer transcription template and RNA polymerase. The expected product is a 4-mer truncated mRNA message of the sequence 5' AGAU 3' (Figure 5.5). UTP ³²P-labeled at the α position is incorporated into this transcript, allowing it to be visualized on a gel. Figure 5.6 shows the results of this experiment. In the absence of SoxR, there are two background transcript bands. The *soxRS* operon present in the template DNA contains two head-to-head promoter sites: that for the *soxS* gene and for *soxR* itself. When SoxR is bound, it represses transcription at its own promoter; thus, the background bands may be indicative of transcription of *soxR*. When oxidized SoxR is bound to the promoter region, the background bands diminish and a strong band appears. This band is attributed to the 4-mer truncated mRNA transcript for *soxS*. The length of this transcript was verified by comparison with a 4-mer DNA marker. These results verify the viability of this transcription assay and that of the SoxR used. This assay, furthermore, is an effective means of testing the quality of future SoxR purifications.

Optimization of transcription assay conditions

The assay was optimized by examining various concentrations of DNA, RNA polymerase, and Mg²⁺. The results are shown in Figure 5.7, with a concern being specificity versus transcript amount. At low concentrations of RNA polymerase (1/500 dilution of the stock), very little transcript is formed. At higher concentrations of RNA polymerase (1/50 dilution of the stock), transcription levels are much higher, with low background transcription. Higher concentrations of Mg²⁺ than normal (see experimental) lead to a decrease of specificity of the polymerase, and increased background transcription.

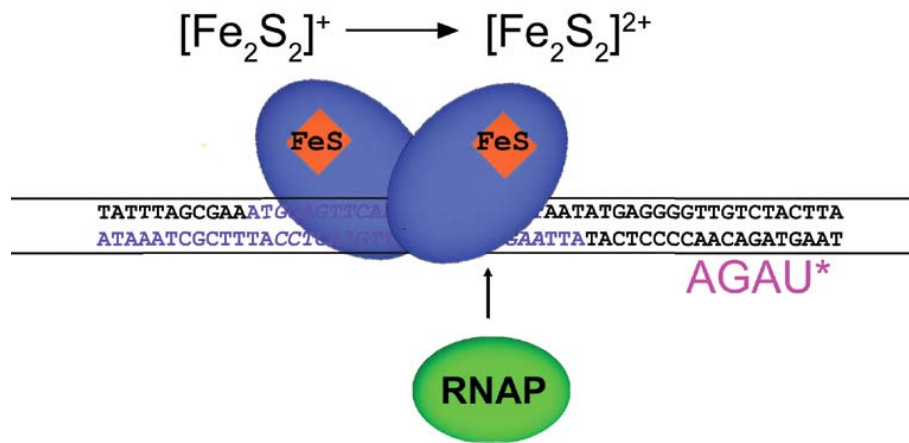


Figure 5.5: A schematic for the abortive transcription assay. SoxR that undergoes a one electron oxidation of one of its [2Fe2S] clusters from the +1 to +2 form is able to recruit RNA polymerase and initiate transcription. The resulting transcript is the radiolabeled mRNA of the sequence ATAU.

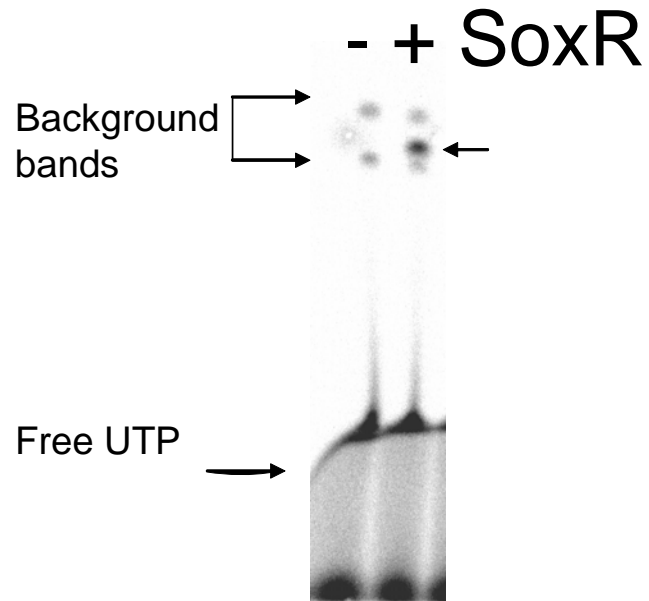


Figure 5.6: SoxR dependent transcription is shown. In the absence of SoxR, two background bands, one of higher and one of lower molecular weight, are present. When oxidized SoxR is present, these background bands diminish and an intense *soxS* transcript fragment is formed. Free radiolabel (UTP) travels faster than the transcript bands, and is not shown in subsequent gels.

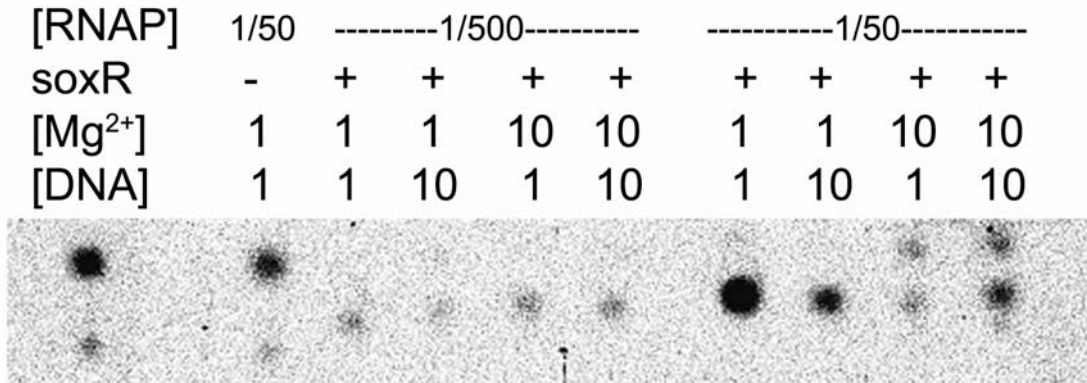


Figure 5.7: Optimization of the concentration of various components of the transcription activation buffer. The numbers indicate the ratio of the concentration to that described under the experimental section. “-” indicates a sample without SoxR; “+” indicates that SoxR was added. High concentrations of RNA polymerase retain specificity with low background while allowing for large amounts of transcription to be seen.

Comparison of P. aeruginosa and E. coli SoxR and effect of irradiation

SoxR from *E. coli* was initially used for these experiments, however, it was discovered that the protein from *Pseudomonas aeruginosa* can functionally complement *E. coli* SoxR, and was shown to be more stable to purification and experimentation. The redox potentials of both these proteins are similar (11). A comparison of transcriptional activity was made for SoxR from both organisms (Figure 5.8). SoxR from *P. aeruginosa* is able to bind and transcribe from the *E. coli soxS* promoter, as the intensity of the transcript bands are similar when SoxR from both organisms is compared. Furthermore, samples containing oxidized SoxR show transcript bands that are more intense than samples containing reduced SoxR. This is the case for the protein from both organisms, demonstrating that the two proteins are equally redox sensitive and are functionally identical.

In addition, samples with the identical components were irradiated for 60 min under the solar simulator, a broad spectrum light source, after which RNA polymerase was added and transcription was allowed to initiate. In all cases, the irradiated samples showed decreased transcription of *soxS*, and increased background transcription, consistent with the protein degrading and dissociating from the promoter site. To prevent protein degradation in future experiments, irradiation was switched to a portable lamp with narrow band-pass filters and a fiber optic output. This allowed for intense irradiation at the excitation wavelength of $[\text{Rh}(\text{phi})_2\text{bpy}]^{3+}$, which in turn required shorter irradiation times.

Light induced transcriptional activation

The optimized transcription assay was used to examine the oxidation of SoxR from a distance, through DNA-mediated charge transport of radicals formed in the transcription template by a covalently tethered photooxidant. This experimental scheme is shown in Figure 5.9. $[\text{Rh}(\text{phi})_2\text{bpy}]^{3+}$, covalently tethered to DNA 80 base pairs away from the site of SoxR binding, is excited by 350 nm light, where it is able to inject a hole into the DNA base stack.

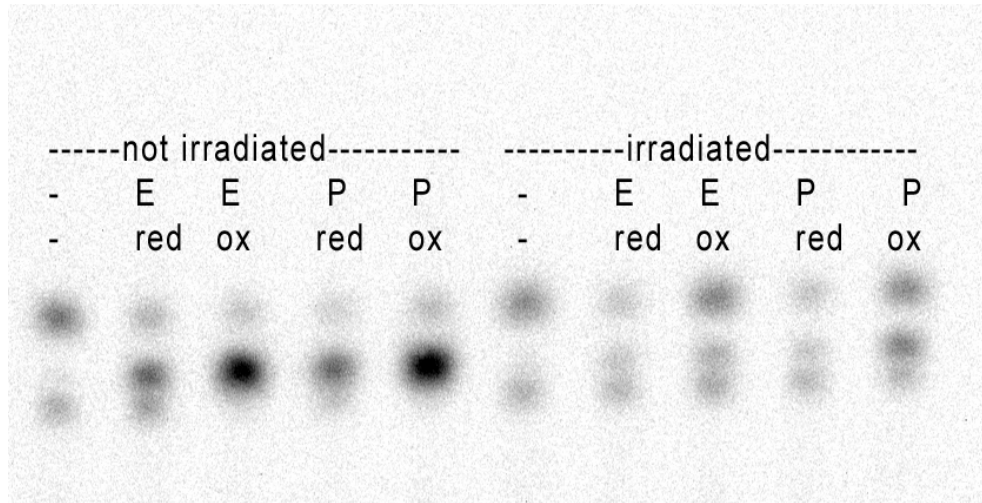


Figure 5.8: Comparison of SoxR from *E. coli* (E) and *P. aeruginosa* (P). “-” indicates a sample without SoxR. Effect of irradiation. SoxR from both organisms shows high transcriptional activity at the *E. coli* SoxR binding region. Reduced SoxR shows diminished transcription over oxidized SoxR; residual transcription is due to incomplete reduction of the protein by dithionite. Irradiation for 60 min under the solar simulator causes SoxR to degrade and fall off the DNA, as indicated by the decrease in the *soxS* transcript and the increase in the background transcription across all samples.

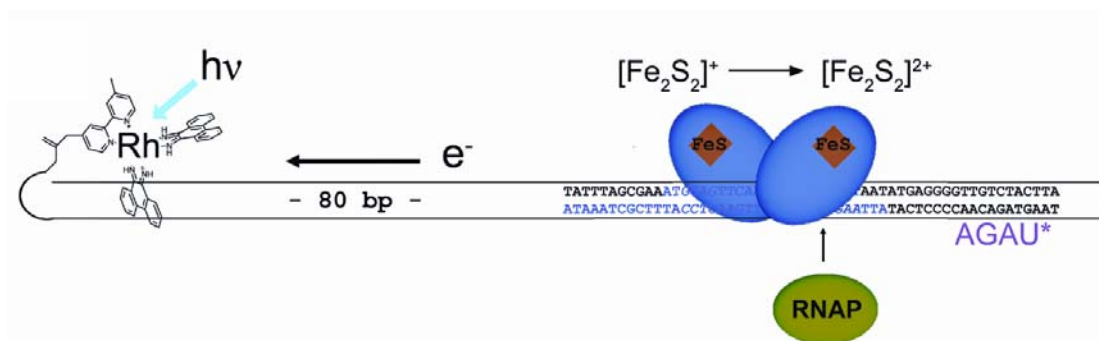


Figure 5.9: Schematic of the SoxR/DNA complex used to carry out the abortive transcription assay. The SoxR binding site is shown in blue. All experiments were carried out anaerobically. Photooxidation of DNA by the covalently tethered $[\text{Rh}(\text{phi})_2\text{bpy}]^{3+}$ oxidizes reduced SoxR bound to DNA. The samples are then incubated with RNA polymerase, and transcription is initiated by addition of a buffer containing a starting dinucleotide, [ApG], ATP, and radiolabeled UTP. The resulting mRNA product is the 4-mer RNA radiolabeled as indicated by the asterisk. Reinitiation of transcription is inhibited by the presence of heparin in the buffer.

The hole localizes at guanine residues in the DNA before reaching the reduced SoxR, which fills the hole by the oxidation of one of its [2Fe2S] clusters from the +1 to the +2 state. Oxidized SoxR bends and unwinds the DNA at its binding site, allowing RNA polymerase to bind and initiate transcription of *soxS*. These experiments are performed in the anaerobic atmosphere inside a glove box to maintain SoxR in its reduced state. The results are seen in Figure 5.10; shown is a representative experiment along with data averaged from several experiments. In the absence of SoxR, only background transcription is seen. With oxidized SoxR, these background bands vanish and a strong band emerges corresponding to the 4-mer transcript. The remaining samples are made with SoxR which has been reduced by the addition of dithionite. When DNA unmodified with [Rh(phi)₂bpy]³⁺ is irradiated (light control, LC), or when the covalently modified DNA is kept in the dark, (dark control, DC), the reduced SoxR cannot be oxidized in a DNA-mediated reaction, and transcription is low. However, when the covalently modified DNA is irradiated, the *soxS* transcript is seen. The amount of *soxS* transcript formed can be correlated to the length of irradiation; longer irradiation lengths allow more holes to be generated, and increased transcription is seen. This effect reaches its maximum between 2 and 3 minutes of irradiation, after which the protein starts to degrade.

DISCUSSION

A transcription assay provides an ideal means of observing the oxidation of SoxR, as it is sensitive, is a turn-on signal, and ensures that SoxR is in a biologically viable state after oxidation. An abortive transcription assay is well suited for this task, as it observes the efficacy of open complex formation and transcriptional initiation by SoxR and RNA polymerase, and allows for a quantitative measure of transcription.

Here, a 180-mer duplex containing the SoxR binding site is PCR amplified using two primers, one of which is covalently modified at the 5'-end with the photooxidant

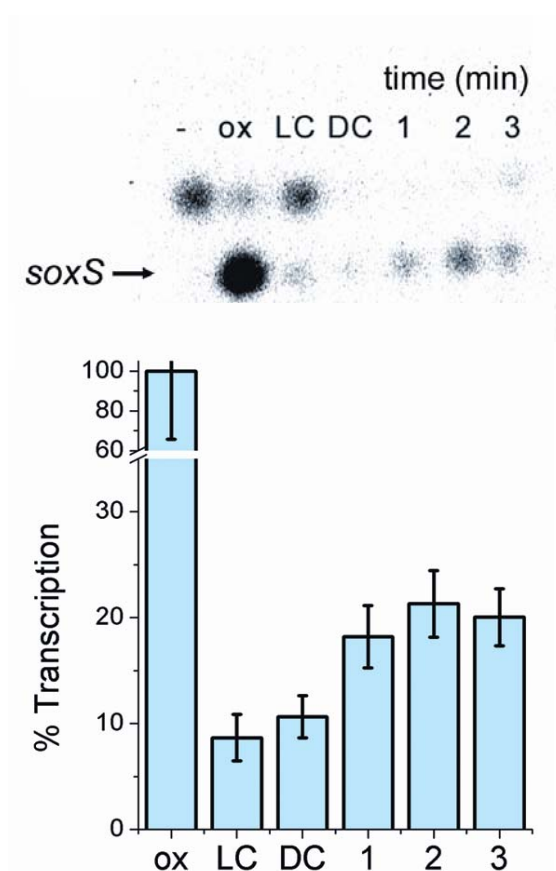


Figure 5.10: Top: Denaturing PAGE of mRNA products of transcriptional activation by SoxR. Shown are the products formed in the absence of SoxR, “-”; in the presence of aerated, oxidized SoxR, “ox”; the DNA template lacking the covalently tethered $[\text{Rh}(\text{phi})_2\text{bpy}]^{3+}$ but with reduced SoxR and irradiated, “LC”, the sample with reduced SoxR and covalent Rh/DNA but without irradiation, “DC”, or with reduced SoxR and covalent Rh/DNA and irradiated for increasing time in minutes, 1, 2, 3; samples treated for longer times gave variable precipitation. The top band reflects background transcription and is inhibited by DNA-bound SoxR; the bottom band is the *soxS* 4-mer transcript. Bottom: Quantitation of *soxS* expression is given as the percent transcription found versus that with fully oxidized SoxR; data were normalized to the background activity in the dark control (DC). The values for the irradiated samples have one-tailed P values versus the light control of 0.106, 0.060, and 0.052 for 1, 2, and 3 min, respectively. The error bars represent the standard error of the average of 4 separate trials.

$[\text{Rh}(\text{phi})_2\text{bpy}]^{3+}$. This photooxidant was chosen as it does not require an external quencher, which could interfere with transcription. The covalent tethering of the complex ensures that it is at the end of the duplex, 80 base pairs away from the site of SoxR binding, making the intervening DNA a necessary medium through which charge must pass.

Examination of guanine oxidation at this 180-mer duplex reveals that damage occurs preferentially at sites which consist of guanine multiplets, and in particular, a 4-guanine site 20 base pairs away from the site of SoxR binding. The overall yield of damage is low, given the short-lived excited state of the Rh photooxidant and its low quantum yield of damage, which is due to rapid back-electron transfer to the long-lived guanine radical (12). Nevertheless, some damage is seen and is not localized near the site of Rh binding, suggesting that the hole equilibrates along the entire length of this DNA. Thus, DNA-mediated CT can occur along a distance long enough to effect SoxR oxidation. In a biological sense, these results highlight the competency of DNA to act as an antenna for oxidative damage in the cell, as the precursor species, oxidative radicals, are able to migrate along the base stack and localize at low potential hot spots that are proximal to the SoxR binding site. Indeed, previous studies have demonstrated that holes formed in DNA are able to be filled oxidation of reduced SoxR (Chapter 3).

Importantly, electrochemistry on SoxR suggests that it undergoes a one-electron oxidation for the dimer. Guanine radicals, whether generated using photooxidants or as a product of naturally occurring oxidative damage, represent one-electron oxidation events. Thus, the transcriptional activation by $[\text{Rh}(\text{phi})_2\text{bpy}]^{3+}$, a one-electron oxidant, as described in this chapter, makes sense in the context of what is known about the oxidation of SoxR.

Hole formation and reduction by reduced SoxR through DNA-mediated charge transport leads to the oxidized, transcriptionally active protein, which can express its target gene. The amount of transcriptional activation seen here is small compared to fully oxidized SoxR, however, reflecting the low quantum yield of DNA damage as described previously for guanine oxidation at the 180-mer duplex. Nonetheless, in the abortive transcription assay used the amount of

mRNA transcript produced is a direct measure of the population of oxidized SoxR generated under these conditions of irradiation and corresponds well to the concentration of guanine radical we expect to have formed. In a cell, SoxR bound to the promoter region would initiate multiple rounds of transcription, thus amplifying the initial damage signal many times. It is interesting to note that these results indicate transcriptional activation from a distance 270 Å away. DNA charge transport provides a means to carry out redox chemistry at long distance.

EXPERIMENTAL

[Rh(phi)₂bpy'] modified primers

[Rh(phi)₂bpy'] was synthesized as described (13). Primer B (5'-GCCACACCGCTG CGTTTCGC- 3') was covalently modified with the photooxidant using the following scheme. DNA was synthesized trityl off, using standard phosphoramidite chemistry on an ABI 3400 DNA synthesizer (Applied Biosystems). The beads were dried and washed with dioxane. Carbonyldiimidazole (CDI, 50 mg, Sigma), was dissolved in 1 mL dioxane, added to beads, and allowed to react with shaking for 30 min. The beads were washed in 3 × 3 mL dioxane. Diaminononane (DAN, 32 mg, Arcos) was dissolved in 1 mL 9:1 dioxane:H₂O, added to the beads, and shaken for 25 min. The beads were washed once with 1 mL 1:10 dioxane:H₂O, twice with 1 mL dioxane, and twice with 1 mL methanol, and dried in air. 1-hydroxybenzotriazole hydrate (HOBt, 1.4 mg, Novabiochem) and 2-(1H-benzotriazol-1-yl)-1,1,3,3-tetramethyluronium hexafluorophosphate (HBTU, 4.4 mg, Novabiochem), were lyophilized for 1 hour to remove residual water and dissolved in 1 mL dimethylformamide (DMF) along with [Rh(phi)₂bpy']Cl₃ (10 mg). Diisopropylethyl amine (DIPEA, 80 µL, Aldrich) was added, forming a deep red solution, which was immediately added to the linker-modified DNA beads. The reaction was allowed to proceed with shaking for 3 hours, after which it was filtered, washed with 2x DMF, methanol, and dried in air. The beads were dissolved in 2 mL NH₄OH, and deprotected at 60°C, vortexing every 15 min for the first hour.

Rh-modified primer was purified via HPLC and stored at 4°C until use. The 180-mer transcription template was made using the Rh-modified primer and primer A (5'-CTGAATAATTTTCTGATGGG-3'). The resulting product was cleaned using a PCR-cleanup kit (Qiagen), checked on an 1.5% agarose gel stained with ethidium bromide, and was quantified using UV-vis spectroscopy.

G^{ox} on the transcription template

The 180-mer transcription template was made using Rh-modified primer B and radiolabeled primer A. Primer A was radiolabeled at the 5' position using polynucleotide kinase (Roche) and [γ -³²P]ATP (labeling grade, MP Biomedical) and purified on a 20% denaturing polyacrylamide gel. Irradiations were carried out using a solar simulator (Oriel Instruments) using a 340 nm internal low-pass filter and a 320 nm external low-pass filter. The resulting DNA was treated with piperidine for one hour, dried under vacuum, and dissolved in loading dye. The DNA fragments were electrophoresed on a denaturing 10% polyacrylamide gel at 90 W for 2 hours, and visualized using autoradiography (GE Healthcare).

Transcriptional studies

The abortive transcription assay was modified from one published previously (6). Transcription activation buffer [6 mM ApG (Dharmacon), 0.1 mM ATP, 0.25 μ M [α -³²P]UTP (>600 Ci/mmol; MP Biomedical), 0.3 M K-glutamate, 30 mM Tris-HCl, pH 8.0, 3 mM MgCl₂, 0.3 mg/mL BSA, 3 mM CaCl₂] was prepared and stored in single use aliquots at -80°C. ApG was deprotected and dried overnight under vacuum, and was added to the transcription activation buffer along with [α -³²P]UTP immediately prior to use. RNA polymerase (1/25 A.U., Epicentre) was diluted according to the supplier's protocols and stored at -80°C until use. Unless otherwise indicated, transcription was carried out using the following conditions. DNA (30 fmol in 15 mM NaPi, 50 mM NaCl) was incubated in 30 μ L 300 nM SoxR (75 mM KCl, 10 mM Tris, 2 mM

MgCl₂, pH 8.0), from *E. coli* or *P. aeruginosa* (6, 11). Reduced samples were prepared using dithionite in an anaerobic chamber. The samples were then irradiated in the glove box using a Schott KL2500 LCD lamp outfitted with the orange filter and at the highest power and iris settings. RNA polymerase was added in a 2 μL volume, and allowed to incubate for 15 min at 35°C. A 10 μL aliquot of this mixture was removed from each sample and replaced with 10 μL transcription activation buffer and samples were allowed to incubate in the glove box for 1 h at 37°C. Reactions were quenched using 3 μL 50 mM EDTA, 30% glycerol, and 8 μL formamide loading buffer. Aliquots (8 μL) were loaded onto a 20% denaturing polyacrylamide gel and electrophoresed at 80 W for 90 min. The gels were visualized using standard autoradiography.

REFERENCES

1. Wu, J.; Dunham, W., Weiss, B. *J. Biol. Chem.* 270:10323-10327 (1995).
2. Gaudu, P.; Moon, N., Weiss, B. *J. Biol. Chem.* 272:5082-5086 (1997).
3. Rhodius, V., Savery, N., Kolb, A., Busby, S. *Methods Mol. Biol.* 2nd. Edition 148:451-464, Humana Press, Totowa, N.J. (2001).
4. Kuraoka, I., Tanaka, K. *Methods Enzymol.* 408:214-223 (2006).
5. Burgess, R. *Annu. Rev. Biochem.* 49:711-740 (1971).
6. Hidalgo E.; Demple, B, *EMBO J.* 13:138-146 (1994).
7. Hidalgo, E. et al *J. Biol Chem.* 270:20908-20914 (1995).
8. Gaudu, P, Weiss, B.; *Proc Natl Acad Sci USA* 93:10094-10098 (1996).
9. Ding, H.; Hidalgo, E.; Demple, B.; *J Biol Chem* 271:33173-33175 (1996).
10. Watanabe S., Kita A., Kobayashi K., Miki K. *Proc. Natl. Acad. Sci. USA.* 105:4121-4126 (2008).
11. Gorodetsky et al. *Proc. Natl. Acad. Sci. USA* 105:3684-3689 (2008).
12. Williams T., Dohno C., Stemp E. D., Barton J. K. *J. Am. Chem. Soc.* 126:8148-8158 (2004).
13. Holmlin R. E., Dandliker P. J., Barton J. K. *Bioconjugate Chem.* 10:1122-1130 (1999).

Chapter 6

Summary and Future Perspectives

Since the discovery of the ability of DNA to conduct charge through its base stack, there has been increasing interest in the ways Nature might be able to exploit this phenomenon. This work seeks to illustrate one such example by demonstrating that the redox-active transcription factor SoxR might use the DNA it is bound to as an antenna to improve its sensitivity to signals from the cellular environment and to facilitate its activation.

These experiments provide one answer as to how SoxR is able to sense oxidative stress and activate the response needed to remediate it while bound to a single site on the genome. Electrochemical studies demonstrate the [2Fe2S] clusters of this protein are able to access the DNA base stack electronically. In cells, the first step in the activation pathway would be the generation of oxidative radicals in DNA by a host of reactive oxygen species that may be present in the cell. Generated radicals would rapidly migrate to areas in the genome of low oxidative potential, such as guanine multiplets, which are found in abundance near the SoxR binding region. Moreover, these one-electron oxidation events in DNA can signal SoxR to become transcriptionally active; DNA-mediated oxidations are exceedingly rapid (on the picosecond to nanosecond timescales) if the species to be oxidized is well coupled into the base stack. Thus oxidative guanine radicals that normally react on a slow (millisecond) timescale to form permanent oxidation products are instead quickly filled by the donation of an electron from reduced SoxR. That these reactions are efficient is evident where the *E. coli* cultures grown in the presence of a known DNA-binding photooxidant and exposed to light induce the expression of *soxS* to an extent comparable to aerated samples with methyl viologen. Importantly, it is also shown here directly that the covalently tethered photooxidant that injects electron holes into the DNA base pair stack can induce the oxidation of SoxR through DNA from a distance to activate transcription. Indeed, these studies present the first direct evidence of transcriptional activation from a distance.

Oxidative stress, in the form of reactive oxygen species or other oxidative insults, threatens cell survival and is implicated in DNA damage, aging, and cancer. It is crucial that cells

are able to detect and respond to conditions of oxidative stress. These results underscore how the DNA duplex can serve as a conduit to signal information regarding cellular stress across the genome. Other studies have identified additional examples of DNA-mediated signaling of oxidative stress: (i) the DNA-mediated oxidation and dissociation of p53 from promoter sites and (ii) the activation of base excision repair proteins by guanine radicals. All these examples illustrate how DNA charge transport can effect redox chemistry without the need for colocalization of redox partners. DNA charge transport chemistry offers a remarkably effective and unique means to achieve long range signaling. Other opportunities where this redox chemistry is utilized within the cell either for transcriptional activation or other regulatory functions should now be considered.